ЖЭТФ, 2003, том 124, вып. 2 (8), стр. 259–287

INSTANTON VERSUS TRADITIONAL WKB APPROACH TO THE LANDAU–ZENER PROBLEM

V. A. Benderskii*

Institute for Problems of Chemical Physics, Russian Academy of Sciences
142432, Chernogolovka, Moscow region, Russia

Laue-Langevin Institute
F-38042, Grenoble, France

E. V. Vetoshkin

Institute for Problems of Chemical Physics, Russian Academy of Sciences
142432, Chernogolovka, Moscow region, Russia

E. I. Kats**

Laue-Langevin Institute
F-38042, Grenoble, France

Landau Institute for Theoretical Physics, Russian Academy of Sciences
142432, Chernogolovka, Moscow region, Russia

Submitted 14 March 2003

Different theoretical approaches to the famous two-state Landau–Zener problem are briefly discussed. Apart from traditional methods of the adiabatic perturbation theory, Born–Oppenheimer approximation with geometric phase effects, two-level approach, and momentum space representation, the problem is treated semiclassically in the coordinate space. In the framework of the instanton approach, we present a full and unified description of the $1D$ Landau–Zener problem of level crossing. The method enables us to treat all four transition points (appearing at two-level crossing) accurately, while the standard WKB approach takes only two of them into account. The latter approximation is adequate for calculating the transition probability or for studying scattering processes, but it does not work in finding the corresponding chemical reactions rates, where all four transition points can often be relevant in the typical range of parameters. Applications of the method and of the results may concern various systems in physics, chemistry, and biology.

PACS: 05.45.-a, 72.10.-d

1. INTRODUCTION

The title of this paper might sound perplexing at first sight. What else can be said about the Landau–Zener (LZ) problem after the numerous descriptions in both research and textbook literature? But although theoretical (and experimental) investigations of different LZ systems began more than seventy years ago, it still remains an active area of research. Various approaches to the LZ problem that have appeared in the literature (see, e.g., the list of publications [1–67], which is by no means complete) are not fully consistent with each other. We therefore think that it is important to discuss all these approaches in a single paper. We study the $1D$ LZ problem [1] of quantum mechanical transitions between the levels of a two-level system at the avoided level crossing. In the LZ theory, a quantum system is placed in a slowly varying external field. Naturally, the system then adiabatically follows variation of an initially prepared discrete state until its time-dependent energy level crosses another level. Near the crossing point, the adiabaticity condition is evidently violated (because the semiclassical behavior

*E-mail: bender@icp.ac.ru
**E-mail: kats@cpd.landau.ac.ru

is violated near turning points). The slow variation of the perturbation implies that the duration of the transition process is very long, and therefore the change in the action during this time is large. In this sense, the LZ problem is a semiclassical one (but with respect to time instead of a coordinate in the standard semiclassical problems).

It is well known that the problem presents the most basic model of nonadiabatic transitions that play a very important role in many fields of physics, chemistry, and biology. It is therefore not surprising that numerous monographs and a great number of papers have been devoted to this subject. In the literature, there are roughly speaking three approaches to semiclassical modeling of the LZ problem,

(i) two-level system approach [2–8],

(ii) adiabatic perturbation theory [9–21] (also see review paper [6]),

(iii) momentum space representation [22–25].

Because different approaches to the LZ problem have been proposed, one of the immediate motivations of the present paper is to develop a uniform and systematic procedure for handling this problem. We show that the three methods listed above are equivalent for treating tunneling and over-barrier regions of parameters, and none of them can be applied, to the intermediate region of parameters where all the four states involved in the LZ system are relevant. To study this region is our main objective in this paper. We also address the so-called connection matrices. In the standard textbook treatment of the LZ problem, only transition probabilities are calculated and expressed in terms of the genuine two-level LZ formula successively applied at each diabatic level intersection. Evidently, such a procedure is an approximation to the general LZ problem, which includes at least four energy levels even in the simplest case. To solve many important physical or chemical problems, one must find the 4×4 (not only 2×2) connection matrices relating these four states.

While this paper is not intended as a comprehensive review, we detail the key results of the standard WKB and instanton approaches from our own research and the literature within the context of different factors that we feel are important in studying the LZ problem. Specifically, we focus in Sec. 2 on the Born–Oppenheimer approximation, which is a benchmark in testing semiclassical approximations. In Sec. 3, we lay the foundation of treating the LZ problem, the adiabatic perturbation theory. Section 4 is devoted to the generalization of the instanton method that enables us to investigate the LZ problem in the momentum space. We show that for a potential that is linear in a $1D$ coordinate under consideration, the WKB semiclassical wave functions in the momentum space coincide with the instanton wave functions. For the quadratically approximated (parabolic) potentials, the instanton wave functions are exact and have no singularities (unlike the WKB wave functions; we recall that relations of the same type hold for the WKB and instanton wave functions in the coordinate space [26–29]).

We advocate the instanton approach in this paper, but it is worth noting that many important results have nevertheless been obtained in the framework of the WKB approach [1–8]. For example, one of the very efficient techniques (the so-called propagator method) was proposed and elaborated by Miller and collaborators [34–36] (also see [26]). This approach uses semiclassic propagators (of the Van Vleck–Gutzwiller type), with the contribution coming from the contour around a complex turning point automatically taken into account in terms of the general WKB formalism. The accuracy of the WKB method can be improved considerably [2, 5, 30, 31] (more recent references on the so-called Laplace contour integration can also be found in [32]) by the appropriate choice of the integration path around the turning point. This method appears to be quite accurate for the tunneling and over-barrier regions, but becomes inadequate in the intermediate energy region. This has been overlooked in the previous investigations treating this region by a simple interpolation from the tunneling region (with a monotonic decay of the transition probability) to the over-barrier region (with oscillating behavior).

In Sec. 5, we present all details of the LZ problem for two electronic states using the instanton description of the LZ problem in the coordinate space. The two basic second-order differential (Schrödinger) equations that we consider are written in the so-called diabatic state representation (i.e., in the basis of «crossed» levels). Neglecting higher-order spatial derivatives, we find asymptotic solutions, and using the adiabatic–diabatic transformation, we match the solutions in the intermediate region. The complete scattering matrix for the LZ problem is derived in Sec. 6. In Sec. 7, we derive the quantization rules for crossing diabatic potentials and briefly discuss the application of the obtained results in some particular models of level crossings that are relevant for the interpretation and description of experimental data on spectroscopy of nonrigid molecules, on inelastic atomic collisions [33], and nonradiative transitions arising from «intersystem» crossings of potential energy surfaces in molecular spectroscopy and chemical dynamics (see, e.g., [26] and references therein). In Sec. 8, we draw our conclusions.

We consider only the $1D$ case in what follows. The LZ problem for 1D potentials coupled to the thermal bath of harmonic oscillators is shown to reduce to a certain renormalization of the Massey parameter, where the longitudinal velocity entering the expression for this parameter is decreased due to the coupling to transverse oscillations (see [26] and references therein, and also [66, 67] for more recent references). Of course, the energy profile of any real system is characterized by a multidimensional surface. But it is often possible to identify a reaction coordinate such that the energy barrier between the initial and final states is minimized along this specific direction, and the system can therefore be effectively treated as $1D$. In certain systems, the physical interpretation of the reaction coordinate is immediate (e.g., the relative bond length in diatomic molecules), but sometimes finding it is not an easy task (if possible at all) because of a large number of possibilities involved. The latter (multidimensional) case will be studied elsewhere. Unfortunately, the accuracy of the WKB method near the barrier top is too poor to make any numbers realistic and it is one more motivation to use a semiclassical formalism alternative to the WKB, namely, the extreme tunneling trajectory or instanton technique.

2. BORN–OPPENHEIMER APPROXIMATION

It may be useful to illustrate the essential physics of the LZ problem starting with a very well known picture corresponding to the Born–Oppenheimer approximation [1, 37]. It leads to the separation of nuclear and electronic motions and is valid only because the electrons are much lighter than the nuclei and therefore move much faster. The small parameter of the Born–Oppenheimer approximation is therefore given by

$$\lambda = \left(\frac{m_e}{m}\right)^{1/4} \ll 1, \tag{2.1}$$

where m_e and m are electronic and nuclear masses respectively. On the other hand, the semiclassical parameter is

$$\gamma = \frac{m\Omega a^2}{\hbar} \gg 1, \tag{2.2}$$

where a is the characteristic length in the problem and $\Omega \propto m^{-1/2}$ is the characteristic nuclear vibration frequency; therefore, $\gamma \propto \lambda^{-2}$. Important conclusions are drawn from this simple fact. Indeed, the semiclassical condition $\gamma \gg 1$ can be satisfied by formally taking $\hbar \to 0$ or equivalently $\lambda \to 0$. This correspondence allows us to apply either the Born–Oppenheimer or the semiclassical approximation to the separation of scales for nuclear and electronic motions on the same footing.

In the traditional Born–Oppenheimer approach, the solution Ψ to the full Schrödinger equation (including the electronic Hamiltonian H_e depending on electronic coordinates r and the nuclear Hamiltonian depending on nuclear coordinates R) is given by an expansion over the electronic Hamiltonian eigenfunctions ϕ_n,

$$\Psi = \sum_n \Phi_n(R)\phi_n(r, R). \tag{2.3}$$

The electronic eigenvalues E_n depend on the nuclear coordinates, and the expansion coefficients $\Phi_n(R)$ are determined by the Born–Oppenheimer equations

$$\left[-\frac{\hbar^2}{2m}\nabla_R^2 + E_n(R) + \frac{\hbar^2}{2m}\sum_{k\neq n} A_{nk}A_{kn} - E\right]\phi_n = \\ = -\frac{\hbar^2}{2m}\sum_{k,m\neq n}(\delta_{nk}\nabla_R - iA_{nk}) \times \\ \times (\delta_{km}\nabla_R - iA_{km})\phi_m, \tag{2.4}$$

where for $m \neq k$,

$$A_{mk} = i\langle\phi_m|\nabla_R\phi_k\rangle, \tag{2.5}$$

and all the diagonal matrix elements $A_{nn} = 0$.

From (2.4), we can find that in the electronic eigenstate E_n, the nuclei move in the effective potential

$$U_n(R) = E_n(R) + \frac{\hbar^2}{2m}\sum_{k\neq n} A_{nk}A_{kn}, \tag{2.6}$$

and transitions between the electronic states n and m are related to the nonadiabatic operator in the right-hand side of (2.4). This simple observation allows us to rewrite effective potential (2.6) as

$$U_n(R) = E_n(R) - \\ - \frac{\hbar^2}{2m}\sum_{m\neq n}\frac{\langle\phi_n|\nabla_R H_e|\phi_m\rangle\langle\phi_m|\nabla_R H_e|\phi_n\rangle}{(E_n - E_m)^2}. \tag{2.7}$$

From this seemingly trivial expression, we derive the following important conclusions:

(i) corrections to E_n have the same order $O(\gamma^{-2})$ as the ratio of the nuclear kinetic energy to the potential;

(ii) off-diagonal matrix elements of the nonadiabatic perturbation operator are also small ($\propto O(\gamma^{-2})$); this fact is formulated as the so-called adiabatic theorem stating that no transitions between unperturbed states occur at adiabatic perturbations ($\lambda \to 0$).

Because the nonadiabatic effects are characterized by the only small parameter γ^{-1} (the semiclassical parameter), they can be described in the framework of semiclassical approaches (e.g., WKB or instanton ones). But we must bear in mind the main problem of the Born–Oppenheimer method: the approximation assumes that the electronic wave functions are real-valued and form a complete basis, but it is impossible to construct such a basis in the entire space including classically accessible and forbidden regions.

If the requirement of a real-valued basis is relaxed, the diagonal matrix elements $A_{nn} \neq 0$, and the effective adiabatic part of the Born–Oppenheimer Hamiltonian takes the form

$$\hat{H}_n = U_n(R) + \frac{\hbar^2}{2m}(\nabla_R - iA_{nn}(R))^2, \tag{2.8}$$

similarly to the Hamiltonian of a charged particle in the magnetic field $B \propto |\nabla_R \times A_{nn}|$. We can therefore change the phases of the electronic and nuclear wave functions as

$$\begin{aligned} &\phi_n \to \phi_n \exp(i\chi_n(R)), \\ &\Phi_n \to \Phi_n \exp(-i\chi_n(R)) \end{aligned} \tag{2.9}$$

by changing the «vector potential» appropriately,

$$A_{nn}(R) \to A_{nn}(R) + \nabla_R \chi_n(R). \tag{2.10}$$

Thus, we confront an important and, at times, mysterious concept of the geometric (or Berry) phase factor that a quantum mechanical wave function acquires upon a cyclic evolution [38–47]. Most characteristic of the concept of the Berry phase is the existence of a continuous parameter space in which the state of the system can travel along a closed path. In our case, the phase is determined by a nonadiabatic interaction (for more details related to the geometric phase for the Born–Oppenheimer systems, see, e.g., review [48]). This phenomenon (which originally manifested itself as a certain extra phase shift appearing upon some external parameter cyclic evolution) has been generalized for the nonadiabatic, noncyclic, and nonunitary cases [49, 50], although most of the Berry phase applications concern the systems undergoing an adiabatic evolution (see, e.g., review [51]). We also note that in addition to the Berry phase, some higher-order corrections to the Born–Oppenheimer approximation also exist (traditionally, and slightly misleadingly called the geometric magnetism or deterministic friction, see [52]). A practically useful application of the Berry phase concept is the energy level displacements predicted in [53] and observed by NMR [54].

The essential physics of these phenomena can be illustrated as follows. There are two subsystems, the fast and the slow ones. The fast subsystem acquires a Berry phase because of the evolution of the slow subsystem. There is a certain feedback effect of the geometric phase on the slow subsystem. As a result, the latter is framed by a gauge field affecting its evolution. The gauge field produces additional (Lorentz-like and electric field-like) forces that must be included into the classical equation of motion. In the case of stochastic external forces (e.g., from surrounding thermal fluctuation media), the Berry phase produces some level broadening for the fast subsystem. In the limit of low temperatures and strong damping, the slow subsystem dynamics can be described by equations of the Langevin type [55]. The general message that we can learn from this fact is that the geometric phases are sources of the dissipative processes for LZ systems.

Thanks to its fundamental origin, this geometric phase has attracted considerable theoretical and experimental attention, but its experimentally observable consequences have been scarce until now. Each opportunity of improving this situation is therefore worth trying. In this respect, the Born–Oppenheimer geometric phase provides a unique opportunity for observation of the geometric phase because it must appear as a nonadiabatic contribution to the standard Bohr–Sommerfeld quantization rule

$$S_n^0 + \chi_n = 2\pi\hbar, \tag{2.11}$$

where S_n^0 is the adiabatic action.

We note that care must be taken when $|E_n(R) - E_m(R)|$ becomes small compared to the characteristic nuclear oscillation energy $\hbar\Omega$. This means that the nonadiabatic interaction energy cannot then be considered as a small perturbation in adiabatic representation (2.4). Fortunately, in the limit

$$|E_n(R) - E_m(R)| < \hbar\Omega,$$

we can start from the other limit with crossing weakly coupled diabatic states and consider the adiabatic coupling as a perturbation. To perform the procedure explicitly, we then need the adiabatic–diabatic transformations

$$\tilde{\Phi}(R) = \exp(i\theta\sigma_y)\Phi(R) \tag{2.12}$$

for the wave functions and

$$\tilde{H} = \exp(i\theta\sigma_y)H\exp(-i\theta\sigma_y) \tag{2.13}$$

for the Hamiltonians, where (H, Φ) and $(\tilde{H}, \tilde{\Phi})$ are the adiabatic and diabatic representations respectively, σ_y is the corresponding Pauli matrix, and θ is

the adiabatic–diabatic transformation parameter (the so-called adiabatic angle).

To illustrate how this works, we consider two coupled crossing effective electronic potentials $U_1(R)$ and $U_2(R)$ (U_{12} is the coupling energy). The corresponding adiabatic and diabatic Hamiltonians are

$$H = -\frac{\hbar^2}{2m}(\nabla_R)^2 + \frac{1}{2}(U_1+U_2) + \left[\frac{1}{2}(U_1-U_2)\cos(2\theta(R)) + U_{12}\sin(2\theta(R))\right]\sigma_3 + \frac{1}{2}\left[-\frac{1}{2}(U_1-U_2)\sin(2\theta(R)) + U_{12}\cos(2\theta(R))\right]\sigma_1, \quad (2.14)$$

and

$$\tilde{H} = -\frac{\hbar^2}{2m}(\nabla_R)^2 + \frac{1}{2}(U_1+U_2) + \frac{1}{2}(U_1-U_2)\sigma_3 U_{12}\sigma_1, \quad (2.15)$$

where $\sigma_{1,2,3}$ are the Pauli matrices and the adiabatic angle is chosen to eliminate the leading interaction term between the adiabatic states,

$$\cos(2\theta(R)) = \frac{U_1-U_2}{2U_{12}}. \quad (2.16)$$

The adiabatic–diabatic transformation can also be brought to a more elegant form [16, 56]

$$(\nabla_R - i\hat{A})\hat{T} = 0, \quad (2.17)$$

where $\hat{T}$ is the sought transformation matrix and the matrix $\hat{A} \equiv A_{nn}$ was introduced above (see (2.5)). The formal solution of Eq. (2.17) can be represented as a contour integral

$$\hat{T}(s) = \hat{T}(s_0)\exp\left(-\int_{s_0}^{s}\hat{A}(s')ds'\right), \quad (2.18)$$

where s_0 and s are the initial and final points of the contour. Solution (2.18) uniquely determines the transformation matrix $\hat{T}$ for a curl-free field $\hat{A}$,

$$\hat{T}(t_0) = \hat{D}\hat{T}(0), \quad (2.19)$$

where the diagonal matrix $\hat{D}$ can be found from (2.17) and is expressed in terms of the geometric phase factor as

$$D_{kn} = \delta_{kn}\exp(i\chi_k). \quad (2.20)$$

Relations (2.11) and (2.20) completely describe the nonadiabatic transitions, the cornerstone of the LZ problem. In addition, (2.11) and (2.20) show that the geometric Born–Oppenheimer phases occur from the diabatic potentials crossing points and enter the quantization rules additively with the contributions from the turning points. Therefore, our main conclusion in this section is that nonadiabatic phenomena must (and can) be included into the general scheme of the semiclassical approach through the corresponding connection matrices [57] (also see [29]) for the appropriate combinations of crossing and turning points in the problem.

3. ADIABATIC PERTURBATION THEORY

It is almost a common student's wisdom nowadays that any solution to the adiabatically time-dependent Schrödinger equation can be represented as an expansion over the complete set of stationary (time-independent) eigenfunctions [1]. In the case under investigation (two-level crossing for the electronic Hamiltonian $H_e(r,t)$), this expansion is given by

$$\Psi(r,t) = c_1(t)\phi_1(r) + c_2(t)\phi_2(r), \quad (3.1)$$

where the wave functions $\phi_{1,2}$ are stationary with respect to a nuclear motion. The time-dependent Schrödinger equation can be exactly rewritten as two first-order equations (with respect to time derivatives) for c_1 and c_2,

$$i\hbar\begin{pmatrix}\dot{c}_1\\ \dot{c}_2\end{pmatrix} = \begin{pmatrix}\tilde{H}_{11} & \tilde{H}_{12}\\ \tilde{H}_{21} & \tilde{H}_{22}\end{pmatrix}\begin{pmatrix}c_1\\ c_2\end{pmatrix}, \quad (3.2)$$

where

$$\tilde{H}_{kk'} = \langle\phi_k|\tilde{H}(t)|\phi_{k'}\rangle, \quad k,k' = 1,2 \quad (3.3)$$

are the matrix elements for the diabatic Hamiltonian.

The phase transformation

$$c_k(t) = a_k(t)\exp\left(-\frac{i}{\hbar}\int\tilde{H}_{kk}(t)dt\right) \quad (3.4)$$

(see, [6, 8, 10]) reduces (3.2) to the coupled first-order equations

$$\begin{aligned} i\hbar\dot{a}_1 &= \tilde{H}_{12}a_2\exp\left(i\int\Omega_{12}(t)dt\right),\\ i\hbar\dot{a}_2 &= \tilde{H}_{21}a_1\exp\left(-i\int\Omega_{12}(t)dt\right), \end{aligned} \quad (3.5)$$

where

$$\Omega_{12} = \frac{1}{\hbar}(\tilde{H}_{22}-\tilde{H}_{11}). \quad (3.6)$$

A slightly different phase transformation

$$c_k(t) = \tilde{\Phi}_k(t) \exp\left(\frac{i}{2\hbar}\int(\tilde{H}_{11}+\tilde{H}_{22})dt\right) \qquad (3.7)$$

preserves the second-order Schrödinger-like form of the equations for the diabatic functions $\tilde{\Phi}_{1,2}$,

$$\hbar^2\frac{d^2\tilde{\Phi}_1}{dt^2} - \left[\left(\frac{\tilde{H}_{11}-\tilde{H}_{22}}{2}\right)^2 + \tilde{H}_{12}\tilde{H}_{21} + \right.$$
$$\left. + \frac{i\hbar}{2}\frac{d}{dt}(\tilde{H}_{11}-\tilde{H}_{22})\right]\tilde{\Phi}_1 = 0. \qquad (3.8)$$

To clarify the mapping of this time-dependent perturbation theory to the two-level crossing problem and the Born–Oppenheimer approach described in Sec. 2, we consider the two-state Born–Oppenheimer equations in the diabatic representation. From (2.15) for one active space coordinate X, we have

$$-\frac{\hbar^2}{2m}\frac{d^2\tilde{\Phi}_1}{dX^2} + (\tilde{H}_{11}-E)\tilde{\Phi}_1 = \tilde{H}_{12}\tilde{\Phi}_2 \qquad (3.9)$$

and

$$-\frac{\hbar^2}{2m}\frac{d^2\tilde{\Phi}_2}{dX^2} + (\tilde{H}_{22}-E)\tilde{\Phi}_2 = \tilde{H}_{21}\tilde{\Phi}_1. \qquad (3.10)$$

If we can neglect the second-order derivatives

$$\frac{\hbar^2}{2m}\frac{d^2\tilde{\Phi}_{1,2}}{dX^2}$$

and replace the time derivative by vd/dX (where $v=\sqrt{2E/m}$ is the velocity), the change of the variables

$$\tilde{\Phi}_{1,2} = \exp(ik_0X)c_{1,2}, \quad k_0^2 = \frac{2mE}{\hbar^2} \qquad (3.11)$$

transforms the two Born–Oppenheimer equations (3.9) and (3.10) into the two level-crossing equations (3.2) for the slow time-dependent perturbations. Obviously, we recognize the standard semiclassical approach in this procedure.

A mapping of the same kind can also be performed for the adiabatic amplitudes $C_{1,2}(t)$ that are related to the diabatic amplitudes $c_{1,2}(t)$ by the adiabatic–diabatic transformation matrix depending on the adiabatic angle θ,

$$\begin{pmatrix} C_1(t) \\ C_2(t) \end{pmatrix} = \begin{pmatrix} \cos\theta & \sin\theta \\ -\sin\theta & \cos\theta \end{pmatrix}\begin{pmatrix} c_1(t) \\ c_2(t) \end{pmatrix}. \qquad (3.12)$$

In the adiabatic basis, we have the set of the first-order equations corresponding to (3.2),

$$\begin{pmatrix} \dot{C}_1 \\ \dot{C}_2 \end{pmatrix} = \begin{pmatrix} H_{11} & -i\dot{\theta} \\ i\dot{\theta} & H_{22} \end{pmatrix}\begin{pmatrix} C_1 \\ C_2 \end{pmatrix}, \qquad (3.13)$$

where the nonadiabatic coupling coefficient $\dot{\theta}$ can be related to the off-diagonal operator A_{12} in (2.5) (or to the geometric phase, see Sec. 2),

$$i\dot{\theta} = A_{12} \equiv i\langle\phi_1|\dot{\phi}_2\rangle. \qquad (3.14)$$

Transformation (3.11) allows reducing the Born–Oppenheimer equations (for the nuclear wave functions $\Phi_{1,2}$ in the adiabatic representation) to (3.13) if and only if the second-order derivatives are neglected (in the spirit of the semiclassical approach) and only $\propto k_0$ terms are kept in the nonadiabatic matrix elements (i.e., higher-order contributions with respect to $1/k_0$ are neglected). Expressions (3.12)–(3.14) do allow an entry point into the adiabatic perturbation theory developed by Landau [1] and Dykhne [10, 11] (also see [15, 16]). We follow the same method closely.

We can make one step further and find the combination of the two-level system amplitudes $a_{1,2}$ in (3.4) and (3.5),

$$Y(t) = \Omega_{12}^{-1/2}\exp\left(-\frac{i}{2}\int\Omega_{12}dt\right)a_1 +$$
$$+ i\Omega_{12}^{-1/2}\exp\left(\frac{i}{2}\int\Omega_{12}dt\right)a_2, \qquad (3.15)$$

satisfying the simple equation

$$\ddot{Y}(t) + \frac{\Omega_{12}^2}{4}Y = 0, \qquad (3.16)$$

which is identical to (3.8) and describes oscillations around the crossing point in the adiabatic potential (inverted adiabatic barrier). In the adiabatic perturbation theory, the level-crossing problem is therefore formally reduced to the well-known quantum mechanical phenomenon, the over-barrier reflection. In the latter problem, moreover, the reflection coefficient is equal to 1, in full agreement with the adiabatic theorem.

Evidently, two adiabatic potentials have no real crossing points in the $1D$ case, and the crossing is therefore possible only at complex values X or t,

$$\Omega_{12}(\tau_c) = 0; \quad U_1 - U_2 = \pm iU_{12}|_{t=\tau_c}. \qquad (3.17)$$

In the vicinity of these points, it follows from (3.6) that

$$\Omega_{12} \propto (t-\tau_c)^{1/2}, \qquad (3.18)$$

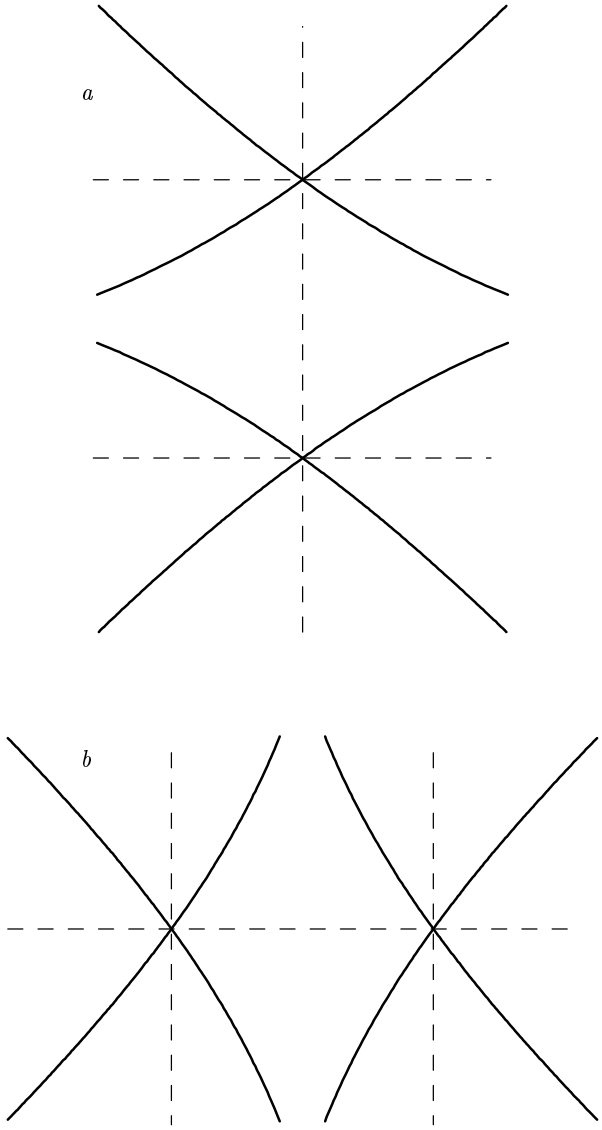

Fig. 1. Stokes (dashed) and anti-Stokes (solid) lines for a pair of close linear turning points replaced by one second-order turning point; a — classically forbidden region, b — classically accessible region

and therefore

$$\int \Omega_{12} dt \approx \frac{2}{3}(t-\tau_c)^{3/2}, \tag{3.19}$$

i.e., the crossing points are square root bifurcation points for the function $\Omega_{12}(t)$. Using (3.19), we depicted the Stokes and anti-Stokes lines for Eq. (3.16) in Fig. 1. The diagram shown in this figure is identical to that corresponding to the semiclassical over-barrier reflection problem with linear turning points under consideration. In the leading approximation, the transition

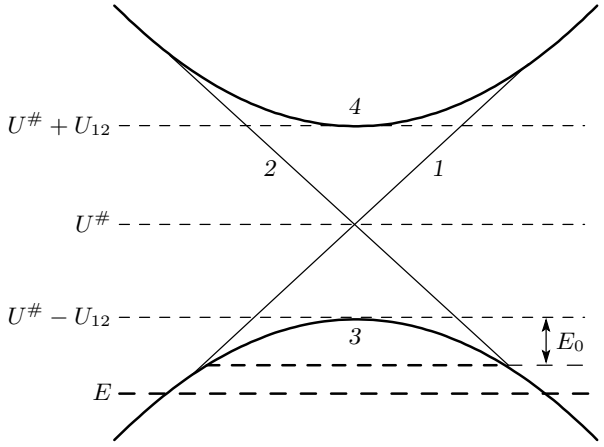

Fig. 2. Adiabatic (3 , 4) and diabatic (1 , 2) potentials for the LZ problem

probability P_{12} is determined by integration over the contour $C(\tau_c)$ going around the bifurcation point τ_c,

$$P_{12} \approx \exp\left\{\frac{2}{\hbar}\oint\limits_{C(\tau_c)} (H_{11}-H_{22})dt\right\}. \tag{3.20}$$

In the simplest form of the LZ problem, the diabatic potentials are assumed to be linear functions of t or X (which is the same because $t = X/v$), see Fig. 2 for illustration,

$$U_{1(2)} = U^{\#} \pm FX. \tag{3.21}$$

Substituting (3.21) in the general expression for the transition probability (3.20), we then find

$$P_{12} \approx \exp(-2\pi\nu), \tag{3.22}$$

where $\nu = U_{12}^2/2\hbar v F$ is the so-called Massey parameter and

$$v = \sqrt{\frac{2|E-U^{\#}|}{m}}$$

is the velocity.

Some comments about the validity range of the approximation are in order. A question of primary importance for the LZ problem is related to the semiclassical nature of the phenomenon. To illustrate this, we note that for

$$\Omega_{12}^2 = U_{12}^2 + v^2F^2X^2,$$

Equation (3.16) is the Weber equation for the real point $X = 0$ (the crossing point of diabatic potentials). Evidently, this correspondence between two complex-conjugate linear crossing points $\pm\tau_c$ and one real crossing point $X = 0$ for the Weber equation is the

same as the correspondence between two linear and one second-order turning points in the standard semiclassical treatment of the Schrödinger equation. We can therefore apply the WKB or instanton methods to the LZ problem in the same way as in any semiclassical problem. We now compare the accuracy of the two approaches. If $|E-U^{\#}| \gg \hbar\Omega$ (where Ω is the characteristic frequency of the adiabatic potentials), the WKB method works quite well if two isolated linear turning points in this problem are considered (this is the limit of $k_0 a \gg 1$, corresponding to the adiabatic approximation). If this is not the case, the diabatic representation must be used.

4. INSTANTON METHOD IN MOMENTUM SPACE

We do not explain the instanton method in detail here and summarize only the most essential points (see [26–29, 58, 59]). The recipe to find the instanton is based on minimizing the classical action functional in the space of paths connecting the minima in the upside-down potential. It is well known [1] that the expansion of an arbitrary wave function $\Psi(x)$ in terms of the momentum eigenfunctions is simply a Fourier integral,

$$\Psi(x) = \frac{1}{2\pi\hbar}\int\limits_{-\infty}^{\infty} \exp\left(\frac{ipx}{\hbar}\right)\Phi(p)dp. \qquad (4.1)$$

The wave function in the momentum representation $\Phi(p)$ can be written in the semiclassical form

$$\Phi(p) = A(p)\exp\left(-\frac{iW(p)}{\hbar}\right), \qquad (4.2)$$

where the action $W(p)$ is determined by the classical trajectory $x_0(p)$ in accordance with the definition

$$\frac{dW}{dp} = x_0(p). \qquad (4.3)$$

We use the dimensionless variables $\epsilon = E/\Omega_0$ for the energy, $V = U/\gamma\Omega_0$ for the potential, and $X = x/a_0$ for the coordinate, where E and U are the corresponding dimensional values of the energy and of the potential, a_0 is a characteristic length of the problem (e.g., the tunneling distance), and Ω_0 is a characteristic frequency (e.g., the oscillation frequency around the potential minimum). The dimensionless momentum can be defined as

$$P = \frac{pa_0}{\gamma\hbar}, \qquad (4.4)$$

where γ is the semiclassical parameter (we recall that $\gamma \equiv m\Omega_0 a_0^2/\hbar$, where m is the mass of the particle, and we believe that $\gamma \gg 1$).

Introducing the semiclassical form (4.2) of the momentum-representation wave function in the standard one-particle $1D$ Schrödinger equation, we can transform it to the form

$$\left[P^2 + 2\hat{V}\left(X_0 + i\frac{1}{\gamma}\frac{d}{dP}\right) - \frac{2}{\gamma}\epsilon\right]A(P) = 0. \qquad (4.5)$$

In the momentum space, $\hat{V}$ is the potential energy operator, which can be expanded in a semiclassical series with respect to $1/\gamma$ (or equivalently, with respect to $\hbar$; we set $\hbar = 1$ in what follows, measuring energies in the units of frequency, except in some intermediate equations where the occurrences of $\hbar$ are necessary for understanding). This expansion allows us to consider $\hat{V}$ as a function V of two independent variables X_0 and d/dP, and we finally obtain

$$V\left(X_0 + \frac{i}{\gamma}\frac{d}{dP}\right) = V(X_0) + \frac{i}{\gamma}\left(\frac{dV}{dX_0}\frac{d}{dP} + \frac{1}{2}\frac{d^2V}{dX_0^2}\frac{dX_0}{dP}\right) + \left(\frac{i}{\gamma}\right)^2\left[\frac{d^2V}{dX_0^2}\frac{d^2}{dP^2} - \frac{1}{2}\frac{d^3V}{dX_0^3}\left(\frac{dX_0}{dP}\frac{d}{dP} - \frac{1}{3}\frac{d^2X_0}{dP^2}\right) + \frac{1}{24}\frac{d^4V}{dX_0^4}\left(\frac{dX_0}{dP}\right)^2\right] + \ldots, \qquad (4.6)$$

where the dots denote all higher-order expansion terms.

In accordance with the general semiclassical rules, we can easily find from (4.5) and (4.6) that the first- and the second-order terms in γ^{-1} become identically zero if the energy-dependent trajectory $X_0(P)$ is determined by the equation

$$P^2 + 2V(X_0) = \frac{2\epsilon}{\gamma} \qquad (4.7)$$

and if the so-called transport equation (TE)

$$\frac{dV}{dX_0}\frac{dA}{dP} + \frac{1}{2}\frac{d^2V}{dX_0^2}\frac{d^2W}{dP^2}A, \qquad (4.8)$$

is also satisfied. The solution of TE (4.8) can be found explicitly as

$$A = \left(\frac{dV}{dX_0}\right)^{-1/2}. \qquad (4.9)$$

It follows from (4.9) that semiclassical WKB wave function (4.2) has singularities at all stationary points of the potential V. These points are therefore turning points in the momentum space. This illustrates fundamental difficulties of the WKB procedure, which consist in matching the solutions that become singular on caustic lines separating manifolds with real and imaginary momenta in phase space.

To also illustrate the second drawback of the WKB method, we consider the linear ($V = FX$) and harmonic ($V = X^2/2$) potentials. The trajectories $X_0(P)$ can be trivially determined from (4.7). For the linear potential, $X_0(P)$ is the inverted parabola with the maximum $X_{0m} = \epsilon F/\gamma$ at $P = 0$. The left and the right branches of the parabola correspond to the opposite motion directions in the classically accessible region $X_0 < X_{0m}$. For the linear potential, the semiclassical WKB wave function in the momentum space,

$$\Phi(P) = \frac{1}{\sqrt{F}} \exp\left\{-\frac{i}{F}\left(\epsilon P - \gamma\frac{P^3}{6}\right)\right\}, \qquad (4.10)$$

is the Fourier transform of the coordinate-space Airy function. For the harmonic potential, the corresponding trajectories (4.7) are ellipses, and the wave functions have the same functional form in both spaces (momentum and coordinate). It is worthwhile to note that although the WKB functions are not exact, the corresponding eigenvalues coincide with the exact quantum mechanical ones.

As we have shown recently [27–29], many important semiclassical problems can be successfully analyzed by the instanton method. Having in mind momentum space in this section, we recall the main ideas of the instanton approach. The first step of the approach derived in [58] and [59] is the so-called Wick rotation of the phase space corresponding to the transformation to imaginary time $t \to -it$. Under the transformation, both potential and kinetic energies change their signs, and the Lagrangian is replaced by the Hamiltonian in the classical equation of motion. In the momentum space, the low-energy instanton wave functions can be constructed using Wick rotation in the momentum space (i.e., the transformation $P \to iP$); in addition, the term with the energy ϵ in (4.7) must be removed from this equation and taken into account in TE (4.8). In the instanton formalism, the trajectory $X_0(P)$ describes zero-energy motion in the classically forbidden region of the momentum space, where the wave function has the form

$$\Phi(P) = \left(\frac{dV}{dX_0}\right)^{-1/2} Q(P) \exp[-\gamma W(P)], \qquad (4.11)$$

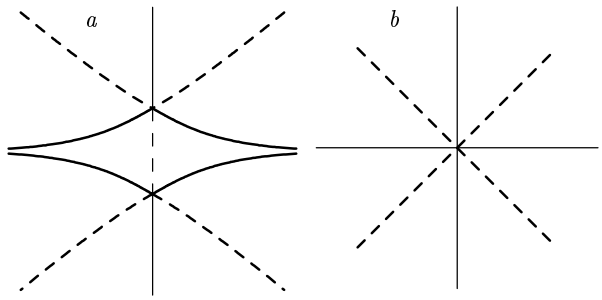

Fig. 3. Stokes (dashed) and anti-Stokes (solid) lines in the vicinity of: (a) conjugate bifurcation points $\pm i\tau_c$; (b) diabatic potentials crossing point $X = 0$

and the additional prefactor $Q(P)$ can be represented as

$$\ln Q(P) = \epsilon \int \left(\frac{dV}{dX_0}\right)^{-1} dP. \qquad (4.12)$$

In the particular case of a linear potential ($V(X) = FX$), the instanton and WKB functions have the same form. For an arbitrary (n-th order) anharmonic potential, the Schrödinger equation in the momentum space is reduced to the n-th order differential equation, but the n-th order derivatives decrease proportionally to γ^{-n}, and the corresponding terms can therefore be taken into account perturbatively. A rigorous mathematical method to perform this procedure (which we use in this paper) has been developed by Fedoryuk [68–70].

To illustrate the instanton approach, we consider the simplest form of the LZ problem illustrated in Fig. 3. For linear potentials with arbitrary line slopes, we have two second-order coupled equations, in the diabatic state representation

$$\begin{aligned} -\frac{d^2\Theta_1}{dX^2} &= \gamma^2(\alpha + f_1 X)\Theta_1 = \gamma^2\nu\Theta_2, \\ -\frac{d^2\Theta_2}{dX^2} &= \gamma^2(\alpha + f_2 X)\Theta_2 = \gamma^2\nu\Theta_1, \end{aligned} \qquad (4.13)$$

where $\Theta_{1,2}$ are the eigenfunctions of the corresponding states and

$$\Omega^2 = \frac{a^2F^2}{mU_{12}}, \quad F = \sqrt{F_1|F_2|}, \quad \gamma = \frac{a^3Fm^{1/2}}{U_{12}^{1/2}},$$

$$\alpha = 2\frac{U_0 - E}{\gamma\Omega}, \quad f_{1,2} = 2\frac{aF_{1,2}}{\gamma\Omega}, \quad \nu = 2\frac{U_{12}}{\gamma\Omega}.$$

Equations (4.13) can be transformed into the momentum space and can then be rewritten as a single second-order equation

$$\frac{d^2\Psi_1}{dk^2} + q(k)\Psi_1(k) = 0, \tag{4.14}$$

where we introduce

$$\Psi_1 = \Phi_1 \exp\left[i\frac{\gamma\alpha^{3/2}}{2}\left(\frac{1}{f_1}+\frac{1}{f_2}\right)\left(k+\frac{k^3}{3}\right)\right], \tag{4.15}$$

Φ_1 is the Fourier transform of Θ_1, $k = P/\gamma\sqrt{\alpha}$, and $q(k)$ is a fourth-order characteristic polynomial

$$q(k) = \lambda^2(1+k^2)^2 + 2\lambda(ik - 2\nu) \tag{4.16}$$

depending on two parameters

$$\lambda = \frac{1}{2}\gamma\alpha^{3/2}\left(\frac{1}{f_1}-\frac{1}{f_2}\right), \quad \nu = \frac{\gamma v^2}{2(f_1-f_2)\sqrt{\alpha}}. \tag{4.17}$$

The first parameter λ plays the role of the new semiclassical parameter in the momentum representation and the second is the known Massey parameter (already defined in (3.22)).

Fortunately, all roots of characteristic polynomial (4.16) can be found analytically quite accurately in the physically most interesting region of parameters. To simplify the expressions (while keeping the complete physical content), we present the results only in the simplest case where $f_1 = -f_2 \equiv f$ (symmetric slopes of the diabatic potentials). In the classically forbidden region $U^{\#} - E > 0$, $\alpha > 0$, at $\lambda \gg 1$ (equivalently, at $\alpha \gg (f/\gamma)^{2/3}$), all the four roots of the polynomial are close to $\pm i$,

$$k_1^{\pm} = i\left(1 \pm \sqrt{\frac{1+\nu}{2\lambda}}\right), \quad k_2^{\pm} = \pm\sqrt{\frac{1-\nu}{2\lambda}} - i. \tag{4.18}$$

In the classically accessible region ($U^{\#} - E < 0$, $\alpha < 0$), the roots are close to ± 1 if $\lambda \gg 1$ (or if $-\alpha \gg (f/\gamma)^{2/3}$),

$$\begin{aligned} k_1^{\pm} &= 1 \pm \left(\frac{\sqrt{1+\tilde\nu^2}+\tilde\nu}{4\tilde\lambda}\right)^{1/2} \pm \\ &\quad \pm i\left(\frac{\sqrt{1+\tilde\nu^2}-\tilde\nu}{4\tilde\lambda}\right)^{1/2}, \\ k_2^{\pm} &= -1 \mp \left(\frac{\sqrt{1+\tilde\nu^2}+\tilde\nu}{4\tilde\lambda}\right)^{1/2} \pm \\ &\quad \pm \left(\frac{\sqrt{1+\tilde\nu^2}-\tilde\nu}{4\tilde\lambda}\right)^{1/2} \end{aligned} \tag{4.19}$$

(the tilde means that in the corresponding quantity, α must be replaced with its modulus).

The roots of characteristic polynomial (4.16) in the classically forbidden region, Eq. (4.18), and in the classically accessible region, Eq. (4.19), are formally equivalent to the transition or turning points for the system of two potential barriers or two potential wells respectively. We can therefore use all the WKB and instanton results known in these cases (see, e.g., our recent paper [29] and references therein for the details). Because only asymptotic solutions and their connections via transition or turning points on the complex plane are usually considered in the semiclassical analysis, the famous Stokes phenomenon [30, 57] of asymptotic solutions plays an essential role, and the distribution of the transition points (which are nothing but the zero points of the characteristic polynomial) and Stokes and anti-Stokes lines determines the phenomenon. We show all the lines emanating from linear turning points in Fig. 2. In the case where the

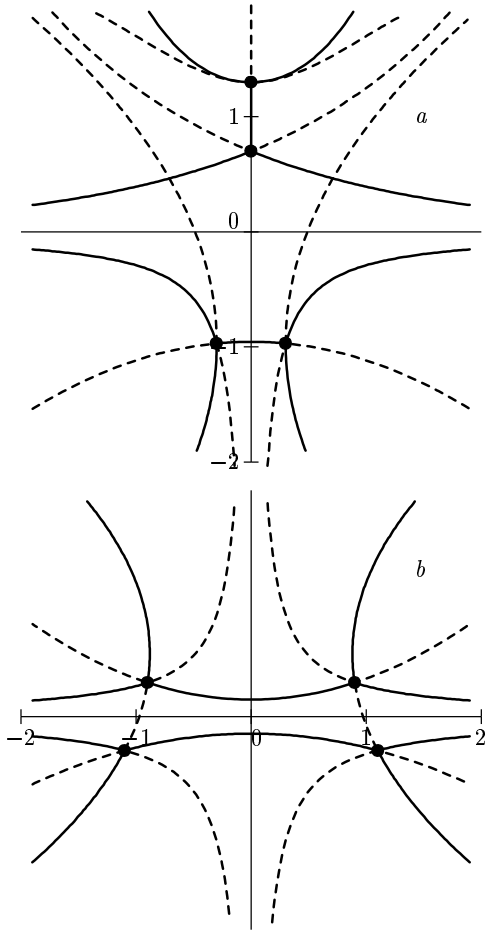

Fig. 4. Stokes (dashed) and anti-Stokes (solid) lines for linear turning points corresponding to classically forbidden (a) and accessible (b) energy regions of the LZ problem

roots form a pair of close linear turning points, every such pair can be replaced with one second-order turning points. The corresponding Stokes and anti-Stokes lines are depicted in Fig. 4.

In the classically forbidden region, the instanton wave functions can be found using roots (4.18),

$$\Phi_1^+ = \frac{(1-ik)^{\nu-1}}{(1+ik)^{\nu+1}} \exp\left[i\lambda\left(k+\frac{k^3}{3}\right)\right],$$
$$\Phi_1^- = \frac{(1-ik)^{-\nu}}{(1+ik)^{-\nu}} \exp\left[-i\lambda\left(k+\frac{k^3}{3}\right)\right]. \tag{4.20}$$

As $|k| \to \infty$, the function Φ_1^+ decreases proportionally to $|k|^{-2}$ and Φ_1^- is reduced to the Airy function [71, 72]. In the vicinity of the second-order turning points $k = \pm i$, the fourth-order characteristic polynomial is reduced to a second-order one, and Eq. (4.14) is reduced to the Weber equation with the known fundamental solutions [71]

$$D_{-\nu}(\pm 2\sqrt{\lambda}(k+i))$$

as $|k+i| \to 0$ and

$$D_{-\nu-1}(\pm 2\sqrt{\lambda}(k-i))$$

as $|k-i| \to 0$. The same procedure applied to the classically accessible region leads to the solutions

$$\Phi_1^+ = \frac{(1-k)^{i\tilde{\nu}-1}}{(1+k)^{i\tilde{\nu}+1}} \exp\left[i\tilde{\lambda}\left(k-\frac{k^3}{3}\right)\right],$$
$$\Phi_1^- = \frac{(1+k)^{i\tilde{\nu}}}{(1-k)^{i\tilde{\nu}}} \exp\left[-i\tilde{\lambda}\left(k-\frac{k^3}{3}\right)\right], \tag{4.21}$$

and it is also reduced to the fundamental solutions of the Weber equation

$$D_{i\tilde{\nu}}\left(\pm 2\sqrt{\tilde{\lambda}}(k+1)\exp\frac{i\pi}{4}\right)$$

as $|k+1| \to 0$ and

$$D_{i\tilde{\nu}-1}\left(\pm 2\sqrt{\tilde{\lambda}}(k-1)\exp\frac{i\pi}{4}\right)$$

as $|k-1| \to 0$.

The same solutions can be obtained for the LZ problem in the two-level approximation using the instanton method in the coordinate space. The reason for this is quite transparent and is based on the fact that for linear diabatic potentials, the limit $k \to \pm\infty$ corresponds to the limit $x \to \pm\infty$, and the asymptotic behaviors of the solutions are therefore the same in the momentum and in the coordinate space.

The entire analysis can be brought into a more compact form by introducing the so-called connection matrices. In the instanton approach, we consider asymptotic solutions and their connections on the complex coordinate plane. It is therefore important to know the connection matrices. The needed connection matrices can easily be found by matching solutions (4.20) or (4.21) at the second-order turning points through the corresponding fundamental solutions of the Weber equation. This gives the connection matrices

$$\hat{M}_1 = \begin{pmatrix} -\cos(\pi\nu) & \dfrac{\sqrt{2\pi}\exp(-2\chi)}{\Gamma(\nu)} \\ \dfrac{\Gamma(\nu)\exp(2\chi)\sin^2(\pi\nu)}{\sqrt{2\pi}} & \cos(\pi\nu) \end{pmatrix}, \tag{4.22}$$

where

$$\chi = \nu - \frac{(\nu-1/2)\ln\nu}{2},$$

and

$$\hat{M}_2 = \begin{pmatrix} -\exp(-\pi\tilde{\nu}) & \dfrac{\sqrt{2\pi}\exp(-\pi\tilde{\nu})\exp(-2\tilde{\chi})}{\Gamma(-i\tilde{\nu})} \\ \dfrac{1}{\sqrt{2\pi}}2\Gamma(-i\tilde{\nu})\exp\left(-\dfrac{\pi\tilde{\nu}}{2}\right)\exp(2\tilde{\chi})\,\mathrm{sh}(\pi\tilde{\nu}) & \exp(-\pi\tilde{\nu}) \end{pmatrix}, \tag{4.23}$$

where

$$\tilde{\chi} = -i\left(\frac{\pi}{4} + \tilde{\nu}(1-\ln\tilde{\nu})\right) + \frac{1}{4}\ln\tilde{\nu}.$$

As a note of caution at the end of this section, we remind the reader that for the linear diabatic potentials, we initially had two corresponding Schrödinger equations, each of which possesses two fundamental solutions. Therefore, the full LZ problem is characterized by four fundamental solutions that are asymptotic to the left of a given turning point and four fundamental solutions that are asymptotic to the right of the same turning point. Generally speaking, the connection matrices must therefore be 4×4 ones. But because of the symmetry of the potentials, these 4×4 matrices have two 2×2 block structures for the functions Φ_1 and Φ_2, given in (4.22) and in (4.23).

5. LZ PROBLEM FOR TWO ELECTRON STATES (INSTANTON APPROACH IN COORDINATE SPACE)

In Secs. 2–4, we investigated the LZ problem in the framework of the adiabatic perturbation theory, the two-level approximation, and the momentum representation. All the three methods are equivalent and semiclassical by their nature, and are therefore applicable in the tunneling and over-barrier energy regions; they become inadequate within the intermediate region (of the order of $\gamma^{-2/3}$) near the level crossing point. The fact is that the accuracy of these methods depends on the «renormalized» (energy-dependent) semiclassical parameter λ in (4.17), which can be small in the intermediate region ($\lambda \leq 1$ even for $\gamma \gg 1$). To treat this region, we must use the coordinate space presentation, because we need to know the connection matrices for nonadiabatic transitions. In the latter problem, the wave functions outside the level crossing point are more convenient (and have a more compact mathematical form) in the coordinate space.

5.1. Tunneling and over-barrier regions

For the smoothness of presentation, we first reproduce the results found in the previous sections for the tunneling and over-barrier energy regions in the coordinate space. In the diabatic representation, we can rewrite two second-order LZ differential equations (4.13) as the fourth-order linear differential equation with constant coefficients at the derivatives

$$\frac{d^4\Phi_1}{dX^4} - 2\gamma^2\alpha\frac{d^2\Phi_1}{dX^2} - 2\gamma^2 f\frac{d\Phi_1}{dX} + \gamma^4(\alpha^2 - v^2 - f^2X^2)\Phi_1 = 0 \quad (5.1)$$

(where we consider the case with a symmetric slope $f_1 = -f_2 \equiv f$ for simplicity). In the mathematical formalism elaborated by Fedoryuk [68–70], Eq. (5.1) is reduced by a semiclassical substitution in a set of equations of the order γ^n. The characteristic polynomial for (5.1) is given by

$$F(\lambda) = \lambda^4 - 2\alpha\gamma^2\lambda^2 - 2\gamma^2 f\lambda + \gamma^4(\alpha^2 - v^2 - f^2X^2), \quad (5.2)$$

where $\lambda = dW/dX$ by definition.

Solving the equation $F(\lambda) = 0$ perturbatively in $\gamma^{-1} \ll 1$, we find

$$\lambda_j = \lambda_j^0 + u_j, \quad (5.3)$$

where

$$\lambda_j^0 = \pm\left[\gamma(\alpha \pm \sqrt{v^2 + f^2X^2})\right]^{1/2} \quad (5.4)$$

and

$$u_j = \frac{\gamma f}{2}\left[(\lambda_j^0)^2 - \alpha\gamma\right]^{-1}. \quad (5.5)$$

Four asymptotic solutions of (5.1) can then be represented as

$$\{y_j\} \equiv \{\Phi_+^+, \Phi_+^-, \Phi_-^+, \Phi_-^-\} = (v^2 + f^2X^2)^{-1/4}\exp\left[\int_0^X \lambda_j(X')dX'\right]. \quad (5.6)$$

They describe the motion with an imaginary momentum in the upper and lower adiabatic potentials

$$\frac{2ma^2}{\hbar^2}\left(U^{\pm} - E\right) = \gamma^2\left(\alpha \pm \sqrt{v^2 + f^2X^2}\right).$$

The subscripts in (5.6) corresponds to the upper or lower adiabatic levels, and the superscripts indicate the sign of the action.

Before considering the connection matrices, we use the substitution

$$\Phi_1 = \exp(\kappa X)\phi, \quad (5.7)$$

and choose the κ value such that the first derivative in (5.1) vanishes,

$$\kappa^3 - \gamma^2\alpha\kappa - \frac{1}{2}\gamma^2 f = 0. \quad (5.8)$$

At $\alpha > 3(f/4\gamma)^{2/3}$, we can expand the roots of (5.8) in terms of the parameter

$$\delta = \frac{f}{4\gamma}\alpha^{-3/2} < \frac{1}{3\sqrt{3}}. \quad (5.9)$$

We thus find

$$\kappa_1 = \gamma\sqrt{\alpha}\left(1+\frac{\delta}{2}\right),$$
$$\kappa_2 = \gamma\sqrt{\alpha}\left(-1+\frac{\delta}{2}\right), \quad \kappa_3 = \gamma\sqrt{\alpha}\delta. \tag{5.10}$$

Under condition (5.9), the coefficients at the fourth and at the third-order derivatives in (5.1) are small (proportional to δ and $\sqrt{\delta}$ respectively) and the fourth-order equation (5.1) can be rewritten as two second-order Weber equations with the solutions

$$D_{p^{(1,2)}}(\beta_{(1,2)}X),$$

where

$$p^1 = -1+\frac{\delta}{2}-\nu\left(1-\frac{3\delta}{2}\right),$$
$$p^2 = \frac{\delta}{2}-\nu\left(1+\frac{3\delta}{2}\right), \tag{5.11}$$
$$\beta_{(1,2)} = \left(\frac{\gamma^2 f^2}{\alpha}\right)^{1/4}\left(1\pm\frac{3\delta}{4}\right).$$

The leading terms of these solutions are the same as those found in Sec. 4. But the Fedoryuk method also gives higher-order corrections in δ in tunneling region (5.8).

In the over-barrier energy region where $\alpha < -3(f/4\gamma)^{2/3}$, the roots of Eq. (5.8) are complex conjugate,

$$\frac{\kappa_{(1,2)}}{\gamma\sqrt{\alpha}} = -\frac{\tilde{\delta}}{2}\pm i\left(1+\frac{3\tilde{\delta}^2}{8}\right), \tag{5.12}$$

and

$$\tilde{\delta} = \frac{f}{4\gamma|\alpha|^{3/2}} \tag{5.13}$$

plays the role of a small parameter. Similarly to the case with the tunneling region, the coefficients at higher-order derivatives are small, and the function ϕ in (5.7) therefore satisfies the Weber equation with the fundamental solutions

$$D_{\tilde{p}^{(1,2)}}(\tilde{\beta}_{(1,2)}X),$$

where

$$\tilde{p}^1 = -1+i\frac{3\tilde{\delta}}{2}+i\nu\left(1+\frac{3\tilde{\delta}}{4}\right),$$
$$\tilde{p}^2 = i\frac{3\tilde{\delta}}{2}+i\nu\left(1-\frac{3\tilde{\delta}}{4}\right),$$
$$\tilde{\beta}_1 = \exp\frac{i\pi}{4}\left(\frac{\gamma^2 f^2}{|\alpha|}\right)^{1/4}, \tag{5.14}$$
$$\tilde{\beta}_2 = \exp\left(-\frac{i3\pi}{4}\right)\left(\frac{\gamma^2 f^2}{|\alpha|}\right)^{1/4}.$$

As was the case with tunneling region (5.11), the leading terms of expansion (5.14) coincide with the results found in the previous sections, but (5.14) also allows computing corrections to the leading terms.

We can now find the connection matrices. To do this in the tunneling region, we must establish the correspondence between solutions of fourth-order differential equation (5.1) and solutions for the states localized in the left (L) and in the right (R) wells. In the case where $\alpha \gg f|X|$, the action can be computed for diabatic potentials starting from both wells (R and L),

$$\gamma W^L \approx \gamma W_0^L + k_0 X + \frac{\beta^2}{4}X^2,$$
$$\gamma W^R \approx \gamma W_0^R - k_0 X + \frac{\beta^2}{4}X^2, \tag{5.15}$$

where

$$k_0 = \left(\frac{2m(U^\# - E)}{\hbar^2}\right)^{1/2} \equiv \gamma\sqrt{\alpha}$$

is the imaginary momentum and $W_0^{L,R}$ are the actions computed from an arbitrary distant point in the L or R wells respectively to the point $X=0$. On the other hand, in the adiabatic potentials

$$U^\pm = U^\# \pm \sqrt{U_{12}^2 + f^2X^2},$$

the corresponding actions can be represented as

$$\gamma W^\pm - \gamma W_0^\pm = k_0 X \pm \frac{\beta^2}{4}X^2\operatorname{sign} X. \tag{5.16}$$

Explicitly comparing the semiclassical wave functions in both representations (adiabatic and diabatic ones), it is easy to see that the adiabatic functions in the potential U^- coincide with the diabatic functions for localized L and R states at $X<0$ and $X>0$ respectively. The adiabatic functions for the upper potential

U^+ correspond to the tails of the diabatic wave functions localized in the opposite wells. In the level crossing region, the L/R diabatic functions are therefore transformed into the R/L functions, and the interaction entangles the diabatic states with the same sign of k_0X. Thus, we have only four nonzero amplitudes of the following transitions:

$$\langle\Phi_L^+|\Phi_R^-\rangle,\ \langle\Phi_L^-|\Phi_R^+\rangle,\ \langle\Phi_R^+|\Phi_L^-\rangle,\ \langle\Phi_R^-|\Phi_L^+\rangle. \qquad (5.17)$$

Recalling that

$$\gamma W^{\pm} = \gamma\int\left(\alpha \pm \sqrt{v^2+f^2X^2}\right)^{1/2} \approx$$

$$\approx k_0X \pm \frac{\beta^2}{4}X^2 \pm \frac{\nu}{2}(1-\ln\nu), \qquad (5.18)$$

we conclude that quantum solutions (5.11), asymptotically valid in the vicinity of the level crossing point, match increasing and decreasing solutions (5.6) smoothly, which leads to the Landau description [1] of the level crossing transitions depicted in Fig. 5.

Using expressions (4.22) and (4.23) relating the fundamental solutions of the Weber equation, we can find the 4×4 connection matrix corresponding to (5.17),

$$\begin{pmatrix}\Phi_R^+\\ \Phi_R^-\\ \Phi_L^+\\ \Phi_L^-\end{pmatrix} = \begin{bmatrix} \dfrac{\sqrt{2\pi}\exp(-2\chi)}{\Gamma(\nu)} & 0 & 0 & -\cos(\pi\nu)\\ 0 & \Gamma(\nu)\exp(2\chi)\sin^2(\pi\nu) & -\cos(\pi\nu) & 0\\ 0 & \cos(\pi\nu) & \dfrac{\sqrt{2\pi}\exp(-2\chi)}{\Gamma(\nu)} & 0\\ \cos(\pi\nu) & 0 & 0 & \dfrac{\Gamma(\nu)\exp(2\chi)\sin^2(\pi\nu)}{\sqrt{2\pi}} \end{bmatrix} \times$$

$$\times \begin{pmatrix}\Phi_L^-\\ \Phi_L^+\\ \Phi_R^-\\ \Phi_R^+\end{pmatrix}, \qquad (5.19)$$

where

$$\chi = \frac{\nu}{2} - \frac{1}{2}\left(\nu-\frac{1}{2}\right)\ln\nu$$

as above. The matrix in (5.19) has a 2×2 block structure, with each of the identical blocks connecting increasing and decreasing diabatic solutions. However, these diagonal blocks do not correspond to the L–R transitions for the lower and upper adiabatic potentials separately. Indeed, the 2×2 matrix corresponding to these transitions is

$$\begin{pmatrix}\Phi_R^+\\ \Phi_L^-\end{pmatrix} = \begin{bmatrix} \dfrac{\sqrt{2\pi}\exp(-2\chi)}{\Gamma(\nu)} & -\cos(\pi\nu)\\ \cos(\pi\nu) & \dfrac{\Gamma(\nu)\exp(2\chi)\sin^2(\pi\nu)}{\sqrt{2\pi}} \end{bmatrix} \times$$

$$\times \begin{pmatrix}\Phi_L^-\\ \Phi_R^+\end{pmatrix}. \qquad (5.20)$$

In the diabatic limit (i.e., as $\nu\to0$) the diagonal matrix elements are small ($\propto\nu^{1/2}$ and $\nu^{3/2}$ respectively), and the off-diagonal elements tend to ±1, as it should be because by definition, there are no transitions between the diabatic potentials.

In the adiabatic limit $\nu\gg1$, the diagonal matrix elements tend to 1, which implies that the decreasing L solution transforms only into the increasing R solution, and vice versa. Therefore, the connection matrix in the tunneling region depends only on the Massey parameter ν. We recall that the blocks of the 4×4 connection matrix in (5.19) correspond to the two isolated second-order turning points with the Stokes constant (see, e.g., [29])

$$T_2 = \frac{\sqrt{2\pi}}{\Gamma(\nu)}\exp(-2\chi). \qquad (5.21)$$

The over-barrier region can be studied similarly. Repeating the procedure described above for the tunneling region (with the evident replacements $k_0\to-ik_0$ and $\beta^2\to i\beta^2$), we obtain the 4×4 connection matrix

$$\hat{U} = \begin{bmatrix} \frac{\sqrt{2\pi}\exp(-2\tilde{\chi})}{\Gamma(-i\nu)} & 0 & 0 & -\exp(-\pi\nu) \\ 0 & \frac{2\Gamma(-i\nu)\exp(-\pi\nu)\exp(2\tilde{\chi})\,\mathrm{sh}(\pi\nu)}{\sqrt{2\pi}} & -\exp(-\pi\nu) & 0 \\ 0 & \exp(-\pi\nu) & \frac{\sqrt{2\pi}\exp(-2\tilde{\chi})}{\Gamma(-i\nu)} & 0 \\ \exp(-\pi\nu) & 0 & 0 & \frac{2\Gamma(-i\nu)\exp(2\tilde{\chi})\exp(-\pi\nu)\,\mathrm{sh}(\pi\nu)}{\sqrt{2\pi}} \end{bmatrix}, \tag{5.22}$$

where

$$\tilde{\chi} = -\frac{i}{2}\left[\frac{\pi}{4} + \nu(1-\ln\nu)\right] + \frac{1}{4}(\pi\nu + \ln\nu). \tag{5.23}$$

As already mentioned for the tunneling region, the blocks in (5.22) correspond to the two isolated second-order turning points with the Stokes constant [29]

$$\tilde{T}_2 = \frac{\sqrt{2\pi}}{\Gamma(-i\nu)}\exp(-2\tilde{\chi}). \tag{5.24}$$

Thus, we arrive at the important conclusion that the main peculiarity of the LZ level crossing (in comparison with the standard, e.g., one-potential problems) is that the second-order turning points characterizing the diabatic level crossing for the LZ problem possesses different Stokes constants T_2, Eq. (5.21), and $\tilde{T}_2$, Eq. (5.24), in the tunneling and in the over-barrier regions.

5.2. Intermediate energy region

We can now reap the fruits of our effort in the previous subsection. We first note that Eqs. (5.11) and (5.14) imply that as the energy approaches the top of the barrier, the exponents $p^{(i)}$ and $\tilde{p}^{(i)}$ of the parabolic cylinder functions increase and therefore more and more deviate from the value prescribed by the Massey parameter ν. Second, $\beta_{(i)}$ increases as $|\alpha|$ decreases, resulting in a decrease of the values of $|X|$ where the asymptotic smooth matching of the solutions must be performed. As $\delta \to 0$, these $|X|$ values are located deeply in the classically forbidden region, where the potentials are close to the diabatic potentials; for $\delta \geq 2\sqrt{3}/3$, these coordinates $|X|$ are of the order of the quantum zero-point oscillation amplitudes, and therefore the adiabatic representation must be used to find the solution in this region.

These two simple observations give us a conjecture how to treat the LZ problem in the intermediate energy region. We must first find the energy «window» for the intermediate region. It is convenient to choose the adiabatic potential frequency $\Omega = F/\sqrt{mU_{12}}$ as the energy scale such that the inequality $|\alpha| < 3|f/4\gamma|^{2/3}$ becomes

$$|U^* - E| \leq \frac{3}{2}U_{12}^{1/3}\left(\frac{\Omega}{2}\right)^{2/3} \equiv U_{12}^*. \tag{5.25}$$

In other words, the characteristic interaction energy at the boundaries of the intermediate region is independent of U_{12}. But the positions of the linear turning points $|X^*|$ corresponding to the energies $U^* \pm U_{12}^*$ depend on the ratio U_{12}/U_{12}^*. These points are located inside or outside the interval $[-a_0\gamma^{-1/2}, a_0\gamma^{-1/2}]$ at $U_{12}/U_{12}^* < 1$ and at $U_{12}/U_{12}^* > 1$, respectively, and the matching conditions in the intermediate energy region are therefore different in the two cases. In the former case, the potentials can be reasonably approximated by a parabola in the asymptotic matching region, and we must therefore work with the Weber equations. In the latter case, the matching is performed in the region where the potentials are linear, and the equations are therefore reduced to the Airy equations.

We first investigate the case where $U_{12}/U_{12}^* > 1$. Using the Born–Oppenheimer approach described in Sec. 2, we see that the Schrödinger equations for the wave functions $\Psi_\pm$ are decoupled in the adiabatic representation with the accuracy up to γ^{-2},

$$-\frac{d^2\Psi_\pm}{dX^2} + \gamma^2\left(\alpha \pm \sqrt{v^2 + f^2X^2}\right)\Psi_\pm = 0. \tag{5.26}$$

For $|X| < v/f$, Eqs. (5.26) are reduced to the Weber equations with the fundamental solutions

$$D_{-1/2-q_1}(\pm\sqrt{2\gamma}X)$$

and

$$D_{-1/2+iq_2}\left(\pm\exp\left(-\frac{i\pi}{4}\right)\sqrt{2\gamma}X\right),$$

where

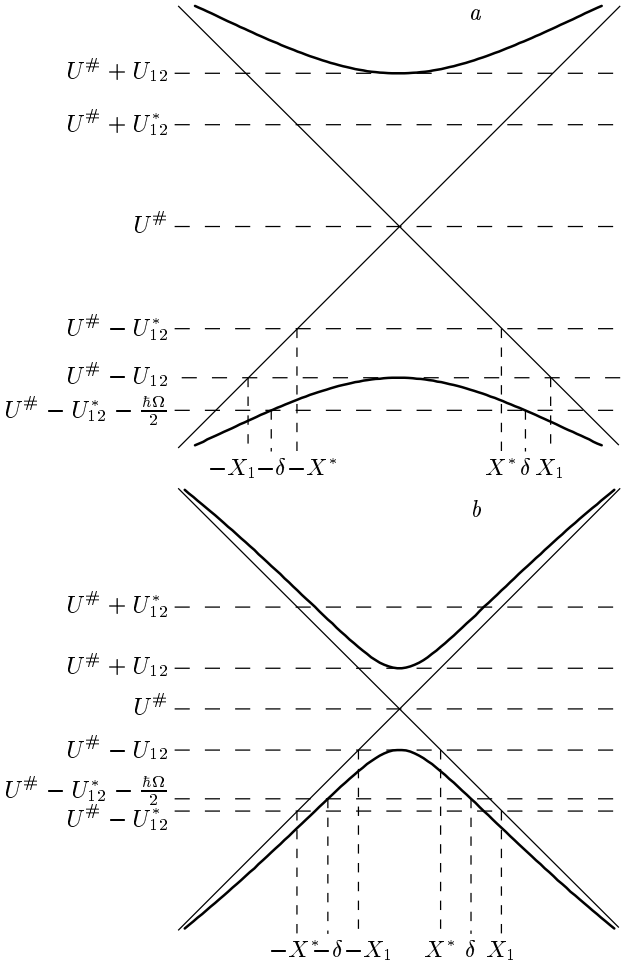

Fig. 5. Relative placement of the adiabatic levels; *a* — $U_{12} > U_{12}^*$, *b* — $U_{12} < U_{12}^*$ ($U_{12}^* \equiv (3/2)(\hbar^2F^2/4m)^{1/3}$)

$$q_1 = \gamma\frac{v+\alpha}{2}, \quad q_2 = \gamma\frac{v-\alpha}{2}, \tag{5.27}$$

are independent of the Massey parameter ν. Two real solutions of (5.26) correspond to the upper adiabatic potential (classically forbidden region), and two complex solutions correspond to the classically allowed motion under the lower adiabatic potential.

The argument of the Weber functions is $\propto X\sqrt{\gamma}$, and under the condition $X < v/f$, their asymptotic expansions determine the interval where the matching is to be performed,

$$\gamma^{-1/2}\left(\frac{U_{12}}{\Omega}\right)^{1/2} > \gamma^{-1/2}. \tag{5.28}$$

This inequality can be satisfied only at $U_{12}/U_{12}^* > 1$, when the intermediate region is sufficiently broad in comparison with Ω. The exponents q_1 and q_2 in Eq. (5.27) are then large, and our aim is to find the explicit asymptotic expansions of solutions in this case. For this, we closely follow the method in [73] (also see monograph [72]), which is in fact an expansion of the fundamental Weber solutions in the small parameters $1/|q_i|$. This method leads to the asymptotic solution of Eq. (5.26) at $X > 0$ given by

$$\begin{aligned}\Psi_+^-(X) &\approx Y_+^{-1/2}(X+Y_+)^{-q_1}\exp(-\gamma XY_+),\\ \Psi_-^-(X) &\approx Y_-^{-1/2}(X+Y_-)^{iq_2}\exp(i\gamma XY_-),\end{aligned} \tag{5.29}$$

where $Y_\pm = \sqrt{v\pm\alpha+X^2}$. Using the known relation between the fundamental solutions of the Weber equation [71, 72],

$$D_\mu(z) = \exp(-i\pi\mu)D_\mu(z) + \\ + \frac{\sqrt{2\pi}}{\Gamma(-\mu)}\exp\left(-i\pi\frac{\mu+1}{2}\right)D_{-\mu-1}(iz),$$

we can find the other two solutions (complementary to (5.29)) as

$$\Psi_+^+(X) = Y_+^{-1/2}\Bigg[-\sin(\pi q_1)(X+Y_+)^{-q_1}\times \\ \times\exp(-\gamma XY_+) + \exp(-2\chi_1)\times \\ \times\frac{\sqrt{2\pi}}{\Gamma(1/2+q_1)}(X+Y_+)^{q_1}\exp(\gamma XY_+)\Bigg], \tag{5.30}$$

and

$$\Psi_-^+(X) = \\ = Y_+^{-1/2}\Bigg[-i\exp(-\pi q_2)(X+Y_-)^{iq_2}\exp(i\gamma XY_-)+ \\ +\exp(-2\chi_2)\frac{\sqrt{2\pi}}{\Gamma(1/2-iq_2)}(X+Y_-)^{iq_2}\times \\ \times\ \exp(-i\gamma XY_-)\Bigg], \tag{5.31}$$

where we introduce the notation

$$\chi_1 = \frac{1}{2}\left(q_1+\frac{1}{2}\right) - \frac{q_1}{2}\ln\left(q_1+\frac{1}{2}\right),$$

$$\chi_2 = -\frac{1}{2}\left(iq_2-\frac{1}{2}\right) + \frac{iq_2}{2}\left[-i\frac{\pi}{2}+\ln\left(q_2+\frac{i}{2}\right)\right].$$

Not surprisingly, solutions (5.29)–(5.31) can be represented as a linear combination of the semiclassical solutions $\Phi_\pm^\pm$ in (5.6) with the coefficients

$$\cos(2\theta_{(1,2)}) = \frac{X}{\sqrt{v\pm\alpha+X^2}}. \tag{5.32}$$

These energy-dependent angles $\theta_{(1,2)}$ coincide with the adiabatic angles introduced above (see (2.12) and (3.12)) at the level crossing point $\alpha = 0$, and $f|X| < v$. Both angles take only slightly different values over the entire intermediate region $|\alpha| < v$.

We can now find all the connection matrices for these functions. Although the calculation is straitforward, it must be done with caution (e.g., because the X-dependent matrices have different functional forms at positive and negative X). For $X > 0$, we obtain

$$\begin{pmatrix} \Psi_-^- \\ \Psi_-^+ \\ \Psi_+^- \\ \Psi_+^+ \end{pmatrix} = \begin{bmatrix} \cos\theta_2 & 0 & 0 & 0 \\ -i\exp(-\pi q_2)\cos\theta_2 & \dfrac{\sqrt{2\pi}\exp(-2\chi_2)\cos\theta_2}{\Gamma(1/2-iq_2)} & 0 & 0 \\ 0 & 0 & \sin\theta_1 & 0 \\ 0 & 0 & -\sin(\pi q_1)\sin\theta_1 & \dfrac{\sqrt{2\pi}\exp(-2\chi_1)\sin\theta_1}{\Gamma(1/2+q_1)} \end{bmatrix} \times \begin{pmatrix} \Phi_-^+ \\ \Phi_-^- \\ \Phi_+^- \\ \Phi_+^+ \end{pmatrix}, \quad (5.33)$$

and for $X < 0$,

$$\begin{pmatrix} \Psi_-^- \\ \Psi_-^+ \\ \Psi_+^- \\ \Psi_+^+ \end{pmatrix} = \begin{bmatrix} \dfrac{\sqrt{2\pi}\exp(-2\chi_2)\cos\theta_2}{\Gamma(1/2-iq_2)} & -i\exp(-\pi q_2)\cos\theta_2 & 0 & 0 \\ 0 & \cos\theta_2 & 0 & 0 \\ 0 & 0 & \dfrac{\sin\theta_1\sqrt{2\pi}\exp(-2\chi_1)}{\Gamma(1/2+q_1)} & -\sin(\pi q_1)\sin\theta_1 \\ 0 & 0 & 0 & \sin\theta_1 \end{bmatrix} \times \begin{pmatrix} \Phi_-^- \\ \Phi_-^+ \\ \Phi_+^+ \\ \Phi_+^- \end{pmatrix}. \quad (5.34)$$

The product of the matrix inverse to (5.33) and the matrix in (5.34) determines the sought connection matrix relating the semiclassical solutions in the intermediate energy region (cf. the connection matrices for the tunneling and over-barrier energy regions in (5.20) and (5.22)). Performing this simple algebra, we finally obtain

$$U_{cross} = \begin{bmatrix} \dfrac{\sqrt{2\pi}\exp(-2\chi_2)}{\Gamma(1/2-iq_2)} & i\exp(-\pi q_2) & 0 & 0 \\ -i\exp(-\pi q_2) & 2\exp(2\chi_2)\Gamma(1/2-iq_2)\operatorname{ch}(\pi q_2) & 0 & 0 \\ 0 & 0 & \dfrac{\sqrt{2\pi}\exp(-2\chi_1)}{\Gamma(1/2+q_1)} & \sin(\pi q_1) \\ 0 & 0 & -\sin(\pi q_1) & \cos^2(\pi q_1)\Gamma(1/2+q_1)\exp(2\chi_1) \end{bmatrix}. \quad (5.35)$$

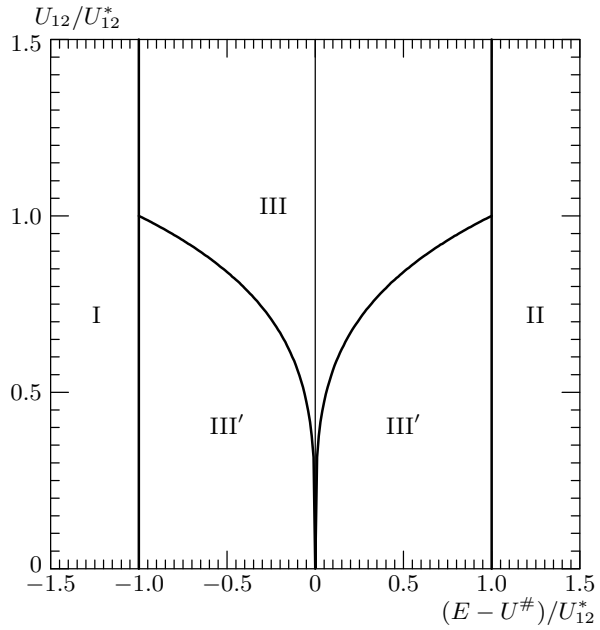

Fig. 6. The E, U_{12} phase diagram (I — tunneling region, II — over-barrier region. The two intermediate energy regions III and III′ are separated by the line $\nu^* = 0.325$)

This matrix has a two 2×2 block structure, similarly to the connection matrices (5.19) and (5.22) for the tunneling and over-barrier regions. But unlike matrices (5.19) and (5.22) describing the transitions between the diabatic states, matrix (5.35) corresponds to transitions between adiabatic states. Indeed, at a strong level coupling ($U_{12} > U_{12}^*$), the eigenfunctions are close to the adiabatic functions and only nonadiabatic perturbations induce transitions. Therefore, the off-diagonal matrix elements in (5.35), which have the meaning of the probability that the diabatic state remains unchanged after the transition, are zero. The block with real-valued matrix elements corresponds to the minimum of the upper adiabatic potential, i.e., to an isolated second-order turning point where [29]

$$q_1 = \frac{U^* - E + U_{12}}{\Omega}. \tag{5.36}$$

The complex-valued block is associated with the maximum of the lower adiabatic potential, and similarly to (5.36), we can find the relation

$$iq_2 = -i\frac{U^* - E + U_{12}}{\Omega} \tag{5.37}$$

for the turning point. For weak level coupling, namely at $|U^* - E| < U_{12}^*$ and $U_{12} < U_{12}^*$ in the intermediate energy region, the adiabatic potentials can be linearized everywhere except a small neighborhood $|X| < v/f \to 0$ of the level crossing point, i.e., can be represented as $\alpha \pm f|X|$. Asymptotic solutions (5.6) are then reduced to a linear combination of the functions

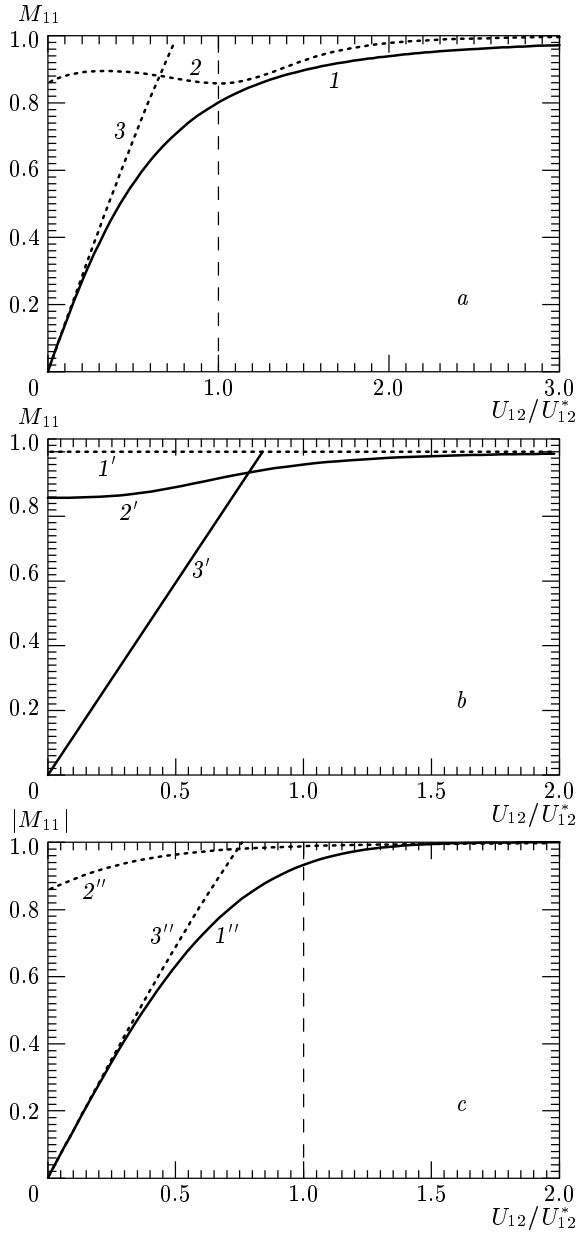

Fig. 7. Transition matrix element M_{11} as a function of U_{12}/U_{12}^*, computed at $\alpha = 0$: on the boundary between tunneling and intermediate energy regions (a); at $E = U^{\#}$ (b), on the boundary between the intermediate and over-barrier regions (c); lines *1*, *2*, *3*, *1′*, *2′*, *3′*, *1″*, *2″*, *3″* are computed for the corresponding energy regions using (5.19), (5.25), and (5.36), respectively

$$\Phi_+^{\pm} \propto (f|X|)^{-1/2} \exp(\pm\xi_+ \operatorname{sign} X),$$
$$\Phi_-^{\pm} \propto (f|X|)^{-1/2} \exp(\pm\xi_- \operatorname{sign} X), \qquad (5.38)$$
$$\xi_{\pm} = \frac{2}{3f}(f|X| \pm \alpha)^{3/2}.$$

All the matrix elements required can now be calculated in the framework of the Landau perturbation theory [1], which can be formulated in terms of the dimensionless variables

$$\tilde{\alpha} = 3 \cdot 2^{-4/3} \frac{U^* - E}{U_{12}}, \quad \tilde{\nu} = 3 \cdot 2^{-4/3} \frac{U_{12}}{U_{12}^*}$$

in order to avoid a divergency of the parameter ν as $\alpha \to 0$. The results of our analysis are shown in Fig. 6. The tunneling and over-barrier regions are separated from the intermediate energy region by the lines $|U_{12}^* - E| = U_{12}^*$. The intermediate region is also split into two parts by the line $\nu = \nu^* = 0.325$, where ν^* is the value of the Massey parameter ν at $U_{12}/U_{12}^* = 1$ and $|U^* - E| = U_{12}^*$. In the region $\nu < \nu^*$, the perturbation theory is an adequate tool for the problem, and the transition matrix elements are proportional to U_{12}/U_{12}^*. At $\nu > \nu^*$, we can use connection matrix (5.35). To illustrate the accuracy of the approximations, we have computed the matrix element M_{11}. The results are shown in Fig. 7. Our computations demonstrate a sufficiently good precision, secured up to two stable digits. The accuracy of the results on the boundaries between the intermediate and over-barrier or tunneling regions is not worse than 3–5 %, and can easily be improved using interpolation approaches.

6. SCATTERING MATRIX

Phenomena of the LZ type can be considered as (and applied to) scattering processes. The expressions for 4×4 connection matrices found in Sec. 5 can be used to calculate the scattering operator (or matrix) $\hat{S}$ that converts an incoming wave into an outgoing one.

We first consider the over-barrier region in the crossing problem with two linear potentials. In this case, in addition to the crossing point chosen as $X = 0$, there are two linear (first-order) turning points $X_0 = \pm|\alpha|/f$ (each turning point for each of the diabatic potentials denoted by L and R). The scattering matrix that relates the asymptotic solutions at $X \ll -X_0$ and $X \gg X_0$ is the product of the 4×4 connection matrix (5.22) and the two known semiclassical connection matrices [57] (also see [29]) describing the wave function evolution from the turning point $-X_0$ to the crossing point 0, and from this point to the turning point $+X_0$, respectively. We thus obtain a 2×2 matrix with the block matrix elements

$$T_{11} = A_{if} \begin{bmatrix} \exp(i(\phi - \phi_0)) & 0 \\ 0 & \exp(-i(\phi - \phi_0)) \end{bmatrix},$$
$$T_{12} = T_{21}^* = (1 - A_{if}^2) \exp \frac{i\gamma W^*}{2} \begin{bmatrix} i & -1/2 \\ -\exp(-i\gamma W^*) & (i/2)\exp(-i\gamma W^*) \end{bmatrix}, \qquad (6.1)$$
$$T_{22} = A_{if} \begin{bmatrix} 2\cos(\gamma W^* - (\phi - \phi_0)) & -\sin(\gamma W^* - (\phi - \phi_0)) \\ \sin(\gamma W^* - (\phi - \phi_0)) & (1/4)\cos(\gamma W^* - (\phi - \phi_0)) \end{bmatrix},$$

where

$$A_{if} = (1 - \exp(-\pi\nu))^{1/2}$$

is the LZ amplitude of the transition between the diabatic states, $\phi - \phi_0 = \tilde{\chi}$ (see (5.23)), and W^* is the action between the linear turning points.

The diagonal elements in (6.1), proportional to the transition amplitude A_{if}, describe propagating waves (i.e., solutions of the Schrödinger equation in the lower adiabatic potential), and the oscillating blocks correspond to solutions in the upper adiabatic potential. Off-diagonal blocks, proportional to the probability that the initial diabatic states remain unchanged, describe the waves reflected from the linear turning points. The reflection (R) and transmission (T) coefficients, interesting in physical applications, can be found from (6.1) by a straightforward calculation,

$$R = -i(1 - A_{if}^2)[A_{if}^2 \exp(i\gamma W^* - 2i(\phi - \phi_0)) +$$
$$+ \exp(-i\gamma W^*)]^{-1},$$
$$T = 2A_{if} \cos(\gamma W^* - (\phi - \phi_0)) \times \qquad (6.2)$$
$$\times [A_{if}^2 \exp(i\gamma W^* - 2i(\phi - \phi_0)) +$$
$$+ \exp(-i\gamma W^*)]^{-1}.$$

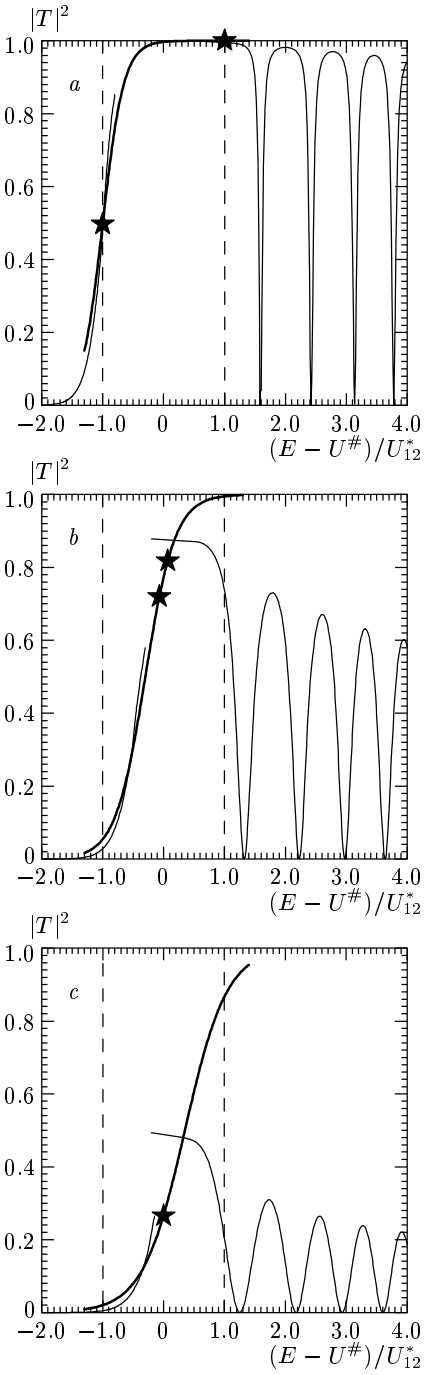

Fig. 8. The T versus E dependence for: (a) $U_{12}=U_{12}^{*}$, (b) $U_{12}=0.5U_{12}^{*}$, (c) $U_{12}=0.25U_{12}^{*}$; stars mark the boundaries of region III′, thin lines show the results for the over-barrier and tunneling regions and bold lines for the intermediate energy region

The poles of the scattering matrix can also be easily found from (6.1), and the corresponding resonance condition is

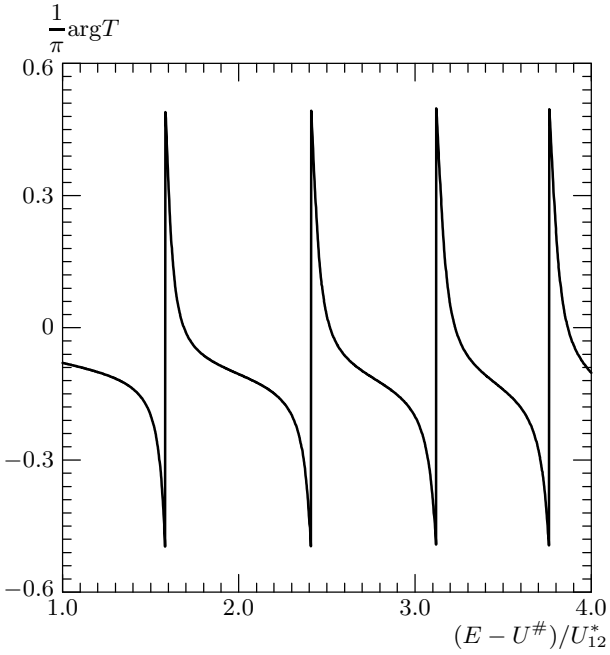

Fig. 9. Transmitted wave phase as a function of E in the over-barrier region at $U_{12}=U_{12}^{*}$

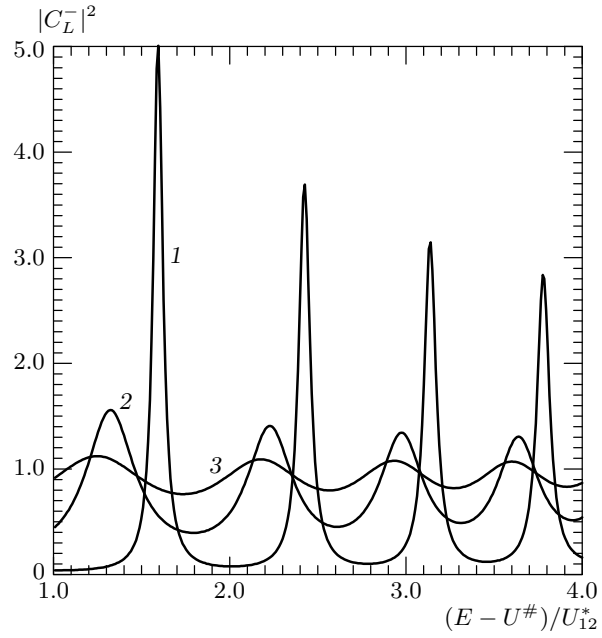

Fig. 10. Amplitudes of the decaying solutions Φ_L^- at $X>0$ versus E for: (1) $U_{12}=U_{12}^{*}$, (2) $U_{12}=0.5U_{12}^{*}$, (3) $U_{12}=0.25U_{12}^{*}$

$$\cos[2(\gamma W^* - (\phi - \phi_0))] =$$

$$= -\left(1 - \frac{1}{2}\exp(-2\pi\nu)\right)(1 - \exp(-2\pi\nu))^{-1/2}. \quad (6.3)$$

The action is complex-valued at the resonance points,

$$\begin{aligned} &\mathrm{Re}(\gamma W^* - (\phi - \phi_0)) = \left(n + \frac{1}{2}\right)\pi, \\ &\mathrm{Im}(\gamma W^* - (\phi - \phi_0)) = -\frac{1}{2}\ln(1 - \exp(-2\pi\nu)). \end{aligned} \quad (6.4)$$

The poles of the scattering matrix are in the lower half-plane of complex E on the vertical lines corresponding to the conventional Bohr–Sommerfeld quantization rules ($\gamma W^* = \pi(n + 1/2)$) for the upper adiabatic potential. In the diabatic limit ($\nu \to 0$), the imaginary part of the pole positions tends to infinity, and in the adiabatic limit ($\nu \to \infty$), the poles move to the real axis. Thus, we see that the eigenstates of the upper adiabatic potential are always quasistationary ones. The resonance widths are determined by the residues of the scattering matrix elements at the poles and can be shown to be monotonically decreasing functions of ν. In Fig. 8, we show the energy dependence of the transmission coefficient T. In the diabatic limit, $T \to 0$, and it increases as U_{12} increases. In the over-barrier region, there appear resonances with the widths Γ_n increasing with the energy increase, because the Massey parameter then decreases and $\Gamma_n \propto \exp(-2\pi\nu)$.

We illustrate the energy dependence of the transmitted wave phase in Fig. 9. In accordance with the general scattering theory [1], there are π-jumps of the phase at each quasidiscrete energy level of the upper adiabatic potential. At $U_{12}/U_{12}^* < 1$, the resonance widths are of the order of the inter-level spacings. The amplitudes of the decaying solutions (localized in the well formed by the upper adiabatic potential) increase near the resonances; this behavior is illustrated in Fig. 10. A primarily important point is that the information about decaying solutions contained in the 4×4 connection matrix (e.g., (5.22)) is lost when we use 2×2 scattering matrix (6.1).

The scattering matrix for the tunneling region can be found by minor modifications of the expression already derived. Instead of matrix (6.1), we thus obtain

$$\begin{aligned} T_{11} &= \begin{bmatrix} (1/4)M_{11}\exp(-\gamma W^*) + M_{22}\exp(\gamma W^*) & i((1/4)M_{11}\exp(-\gamma W^*) - M_{22}\exp(\gamma W^*)) \\ -i((1/4)M_{11}\exp(-\gamma W^*) - M_{22}\exp(\gamma W^*)) & (1/4)M_{11}\exp(-\gamma W^*) + M_{22}\exp(\gamma W^*) \end{bmatrix}, \\ T_{12} &= T_{21}^* = \cos(\pi\nu)\exp\frac{i\gamma W^*}{2}\begin{bmatrix} i & -(1/2)\exp(-\gamma W^*) \\ -1 & (i/2)\exp(-\gamma W^*) \end{bmatrix}, \\ T_{22} &= \begin{bmatrix} M_{11} & 0 \\ 0 & M_{22} \end{bmatrix}, \end{aligned} \quad (6.5)$$

where M_{11} and M_{22} are the corresponding matrix elements from (5.19).

We also compute the reflection and transmission coefficients

$$\begin{aligned} R &= -i\left[\exp(\gamma W^*) - \frac{1}{4}M_{11}^2\exp(-\gamma W^*)\right]\left[\exp(\gamma W^*) + \frac{1}{4}M_{11}^2\exp(-\gamma W^*)\right]^{-1}, \\ T &= M_{11}\left[\exp(\gamma W^*) + \frac{1}{4}M_{11}^2\exp(-\gamma W^*)\right]^{-1}. \end{aligned} \quad (6.6)$$

In the intermediate energy region, the only block matrix element T_{11} requires a special calculation taking the contributions from the complex turning points into account,

$$T_{11} = \begin{bmatrix} \dfrac{\sqrt{2\pi}\exp(-\pi q_2/2)}{\Gamma(1/2 - iq_2)} & i\exp(-\pi q_2) \\ -i\exp(-\pi q_2) & \dfrac{2\Gamma(1/2 - iq_2)\exp(-\pi q_2/2)\,\mathrm{ch}(\pi q_2)}{\sqrt{2\pi}} \end{bmatrix}. \quad (6.7)$$

The other matrix elements are the same as in (5.34). Finally, we also find the reflection and the transmission coefficients in the intermediate energy region,

$$R = \frac{\exp(-\pi q_2)}{\sqrt{1+\exp(-2\pi q_2)}} \exp\left[-i\left(\phi - \frac{\pi}{2}\right)\right],$$
$$T = \frac{1}{\sqrt{1+\exp(-2\pi q_2)}} \exp(-i\phi), \tag{6.8}$$

where $\phi = \arg[\Gamma(1/2 - iq_2)]$.

7. QUANTIZATION RULES FOR CROSSING DIABATIC POTENTIALS

Although instanton trajectories are rather simple objects and can relatively easily be found analytically, calculations of the quantization rules within the instanton approach are rather involved and require the knowledge of the scattering matrix and all the connection matrices calculated in the previous sections. In this section, we apply these results to find the quantization rules for the crossing diabatic potentials shown in Fig. 11. Depending on the Massey parameter, the situations shown in the figure exhaust all cases practically relevant for spectroscopy of nonrigid molecules (symmetric or asymmetric double-well and decaying potentials).

Within the instanton approach, the quantization rule can be formulated as the vanishing condition for the amplitudes of the solutions Φ_L^+ and Φ_R^+ that exponentially increase at $X > 0$ and $X < 0$, respectively. Taking into account that $W_L^* = W_R^*$ (the actions in the corresponding wells of the lower adiabatic potential) and using connection matrix (5.19), we obtain the quantization rule

$$\mathrm{tg}(\gamma W_L^*) = \pm\frac{2}{p}\exp(\gamma W_B^*), \tag{7.1}$$

where W_B^* is the action in the barrier formed in the lower adiabatic potential and $p \equiv U_{11}$ is the corresponding matrix element of connection matrix (5.19).

Quantization condition (7.1) differs from the well-known [1] quantization rule for the symmetric double-well potential only by the factor $1/p$ varying from 0 to 1 in the diabatic and adiabatic limits. Therefore, the tunneling splitting at finite values of the Massey parameter ν can be represented as the product

$$\Delta_n = \Delta_n^0\, p(\nu) \tag{7.2}$$

of the tunneling splitting Δ_n^0 in the adiabatic potential and the factor

$$p(\nu) = \frac{\sqrt{2\pi}}{\Gamma(\nu)}\gamma^{\nu-1/2}\exp(-\nu) \tag{7.3}$$

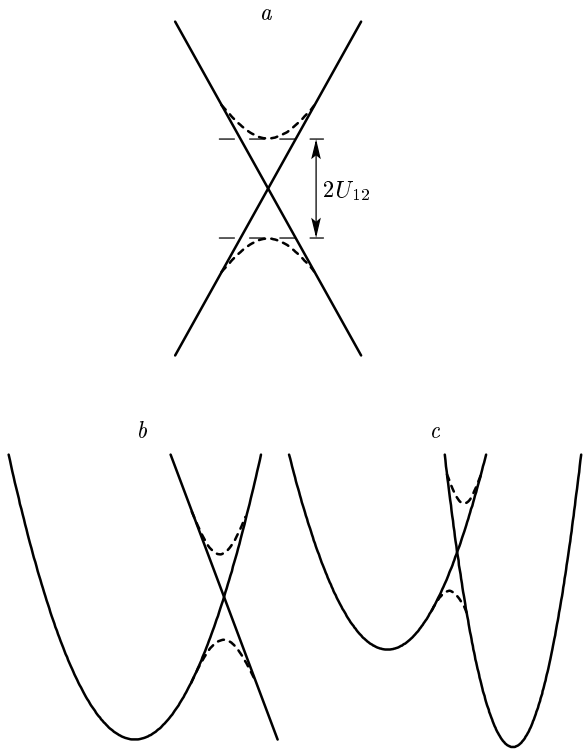

Fig. 11. The diabatic level crossing phenomena: a — crossing region, b — bound initial and decay final states, c — bound initial and final states

associated with the transition amplitudes between the diabatic potentials in the crossing region.

It is particularly instructive to consider (7.1) as the standard [1] Bohr–Sommerfeld quantization rule, with both the geometric φ_n and tunneling χ_n phases included additively in the right-hand side. In the adiabatic limit $p(\nu) \to 1$, we find that $\varphi_n \to 0$ and (7.1) reduces to the quantization of the symmetric double-well potential. In the diabatic limit, $\varphi_n = -\chi_n$ and the geometric phase compensates the tunneling one. The physical argument leading to this compensation can easily be rationalized as follows. At the reflection at the crossing point $X = 0$, the trajectories in the classically forbidden energy region are the same as those for the tunneling region but with the phase shift π.

We now focus on quantization rules for the over-barrier energy region. Closely following the above analysis for the tunneling region (replacing connection matrix (5.19) by matrix (5.22) and making some other self-evident replacements), after some tedious algebra we finally obtain the quantization rule

$$(1-\exp(-2\pi\nu))\cos(2\gamma W_L^* + (\phi-\phi_0)) \times \\ \times \cos(\gamma W^* - (\phi-\phi_0)) + \\ + \exp(-2\pi\nu)\cos^2\left(\gamma W_L^* + \frac{\gamma W^*}{2}\right) = 0, \quad (7.4)$$

where W^* is the action in the well formed by the upper adiabatic potential and $\phi - \phi_0 = \tilde{\chi}$ is determined from (5.23). Equation (7.4) implies that the eigenstates are determined by the parameter

$$B = \frac{\exp(-2\pi\nu)}{1-\exp(-2\pi\nu)}. \quad (7.5)$$

In the diabatic limit $\nu \to 0$, and hence $B \to 1/(2\pi\nu)$, the main contribution to (7.4) is due to the second term, which leads to a splitting of degenerate levels in the diabatic potentials. Moreover, because

$$\gamma\left(W_L^* + \frac{W^*}{2}\right) = \pi\left\{n + \frac{1}{2} \pm \right. \\ \left. \pm 2\nu \sin\left[\gamma\left(W_L^* + \frac{W^*}{2}\right) - \phi + \phi_0\right]\right\}, \quad (7.6)$$

the splitting increases as the Massey parameter ν increases; the splitting is an oscillating function of the interaction U_{12}.

In the adiabatic limit, as $\nu \to \infty$, $\phi - \phi_0 \to 0$, and therefore $B \approx \exp(-2\pi\nu)$ in accordance with (7.5), the main contribution to (7.4) comes from the first term, which determines the quantization rule for the upper one-well potential and for the lower double-well potential in the over-barrier energy region. In this limit, the parameter B plays the role of the tunneling transition matrix element. For B smaller than the nearest level spacings for the lower and upper potentials, we can find two sets of quantization rules from (7.4) that lead to two sets of independent energy levels

$$\gamma W^* = \pi\left(n_1 + \frac{1}{2}\right), \quad 2\gamma W_L^* = \pi\left(n_2 + \frac{1}{2}\right). \quad (7.7)$$

Because the eigenstate energy level displacements depend on U_{12}, resonances can occur at certain values of this parameter, where the independent quantization rules in (7.7) are not correct any more. The widths of these resonances are proportional to $\exp(-2\pi\nu)$ and are therefore strongly diminished as the Massey parameter ν increases. This behavior is easily understood, because the wave functions of the excited states for the lower potential are delocalized in the limit, and their amplitudes in the localization regions for the low-energy states of the upper potential are very small.

A more complicated problem is to derive the quantization rule in the intermediate energy region. We must use connection matrix (5.35) and take the contributions from the imaginary turning points into account. Nevertheless, the quantization rule can finally be written in the simple and compact form

$$\cos(2\gamma W_L^*) = -\exp(-\pi q_2), \quad (7.8)$$

where $q_2 = \gamma(v-\alpha)/2$ is determined by (5.27).

It is useful to illustrate the essence of the general result given above by simple (but nontrivial) examples. We first consider two identical parabolic potentials with their minima at $X = \pm 1$ and with the coupling that does not depend on X. Because of the symmetry, solutions of the Schrödinger equation in this case can be represented as symmetric and antisymmetric combinations of the localized functions

$$\Psi^{\pm} = \frac{1}{\sqrt{2}}(\Phi_L \pm \Phi_R). \quad (7.9)$$

The functions are orthogonal, and in addition, the two sets of functions (Ψ_e^+, Ψ_0^-) and (Ψ_0^+, Ψ_e^-) (where the

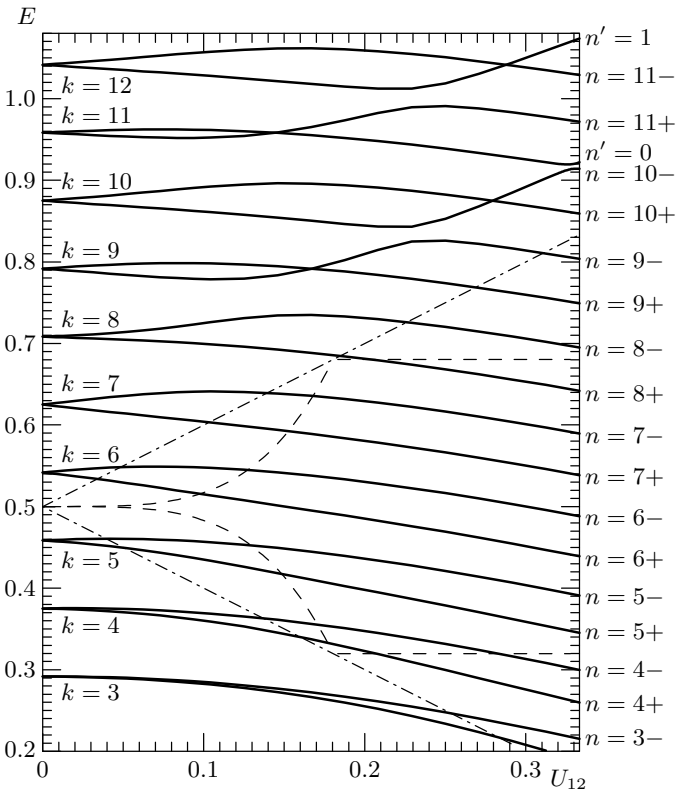

Fig. 12. Level displacements versus U_{12} for two diabatic crossing potentials $(1 \pm X)^2/2$. Dashed lines show the intermediate energy region, dotted-dashed lines show displacements for the top and for the bottom of the adiabatic potentials. k, n, and n' are quantum numbers for the diabatic, lower adiabatic, and upper adiabatic potentials

respective subscripts 0 and e denote the ground and the first excited states) correspond to the two possible types of level crossings.

In Fig. 12, we schematically depict the dependence of the level positions on the coupling U_{12}. In the energy region $E \le U^* + U_{12}$, where only discrete levels of the lower adiabatic potentials exist, there are pairs of the alternating parity levels (Ψ_e^+, Ψ_0^-) and (Ψ_0^+, Ψ_e^-). The tunneling splittings increase monotonically because the Massey parameter ν increases, and the barrier decreases with U_{12}. The same level and parity classification remains correct for the energy region above the barrier of the lower adiabatic potential, where the spectrum becomes almost equidistant. But in the over-barrier region, the resonances occur between levels of the same parity; the sequence of the odd and of the even levels is broken, and level displacements are not monotonic functions of U_{12}. Some of the levels of different parities can pairwise cross. For the upper adiabatic potential, the level sequence is opposite to that for the lower adiabatic potential. We have checked the results of our semiclassical approach and found a remarkably good agreement with the numerical quantum diagonalization.

The second instructive example involves the crossing of one-well and linear diabatic potentials. It leads to the lower adiabatic decay potential and to the upper one-well adiabatic potential. The quantization rules then correspond to the vanishing amplitudes for the exponentially increasing solutions as $X \to -\infty$; in additon, we must require that no waves propagate from the region of infinite motion, i.e., the region $X > 1/2$. Performing the same procedure as above, we find that in the tunneling energy region, the eigenstates are the roots of the equation

$$\mathrm{tg}(\gamma W_L^*) = -i\frac{4}{p^2(\nu)}\exp(2\gamma W_B^*), \tag{7.10}$$

with the same notation as above.

To proceed further, it is convenient to introduce a complex action to describe quasistationary states,

$$\gamma W_L^* = \pi\left(\frac{E_n}{\Omega} - i\frac{\Gamma_n}{2\Omega}\right), \tag{7.11}$$

where $\Omega = \partial W_L/\partial E$ is evidently independent of E. The real and imaginary parts of the quantized eigenstates determined from (7.11) are given by

$$\begin{aligned} E_n &= \Omega\left(n + \frac{1}{2}\right), \\ \Gamma_n &= p^2(\nu)\frac{\Omega}{2\pi}\exp(-2\gamma W_B^*). \end{aligned} \tag{7.12}$$

This relation describes the nonadiabatic tunneling decay of quasistationary states of the lower adiabatic potential. Similarly to the case with the crossing of two parabolic potentials, Eq. (7.2), the tunneling and the adiabatic factors here enter the decay rate multiplicatively. Because the decay rate is proportional to the square of the tunneling matrix element, we have $\Gamma_n \propto p^2(\nu)$, as it should be.

In the over-barrier energy region, the quantization rule is

$$\begin{aligned} &(1 - \exp(-2\pi\nu)\exp[-i(\gamma W_L^* + \phi - \phi_0)] \times \\ &\qquad \times \cos(\gamma W^* - \phi + \phi_0) + \exp(-2\pi\nu) \times \\ &\times \exp\left(-\frac{i\gamma W^*}{2}\right)\cos\left(\gamma W_L^* + \frac{\gamma W^*}{2}\right) = 0, \end{aligned} \tag{7.13}$$

and the actions depend on the energy E as

$$\gamma W_L^* = \pi\frac{E}{\Omega}, \quad \gamma W = \pi\left(-\frac{U^* + U_{12}}{\Omega_1} + \frac{E}{\Omega_1}\right), \tag{7.14}$$

where Ω and Ω_1 are E-dependent frequencies of the diabatic and the upper adiabatic potentials.

In the diabatic limit, the decay rate is proportional to the Massey parameter and is given by

$$\Gamma_n \approx \pi\nu\cos^2(\gamma W - \phi + \phi_0). \tag{7.15}$$

In the opposite, adiabatic limit, the decay rate is

$$\Gamma_n \approx \exp(-2\pi\nu)[1 - \sin(2\gamma W_L^* + \phi - \phi_0)]. \tag{7.16}$$

In both limits, the decay rate is an oscillating function of U_{12}. We illustrate the dependence $\Gamma(U_{12})$ for the crossing diabatic potentials $U_1 = (1 + X)^2/2$ and $U_2 = 1/2 - X$ in Fig. 13. We note that while the tunneling decay rate of low-energy states increases monotonically with the Massey parameter ν, the decay rate of highly excited states tends to zero in both (diabatic and adiabatic) limits. There are certain characteristic values of U_{12} at which the right-hand side of (7.15) or (7.16) vanishes, and therefore $\Gamma_n = 0$.

The last, more general example that we consider in this section describes two nonsymmetric potentials crossing at $X = 0$,

$$U_1 = \frac{1}{2}(1 + X)^2, \quad U_2 = \frac{1}{2b}(X^2 - 2bX + b). \tag{7.17}$$

In a certain sense, this is the generic case, and as the parameter b entering potential (7.17) varies from 1 to ∞, we recover the two particular examples considered above and pass from two identical parabolic potentials to the crossing of the one-well and linear diabatic potentials. Potentials U_2 of this type were recently investigated by two of the authors (V. B. and E. K.) [64] with

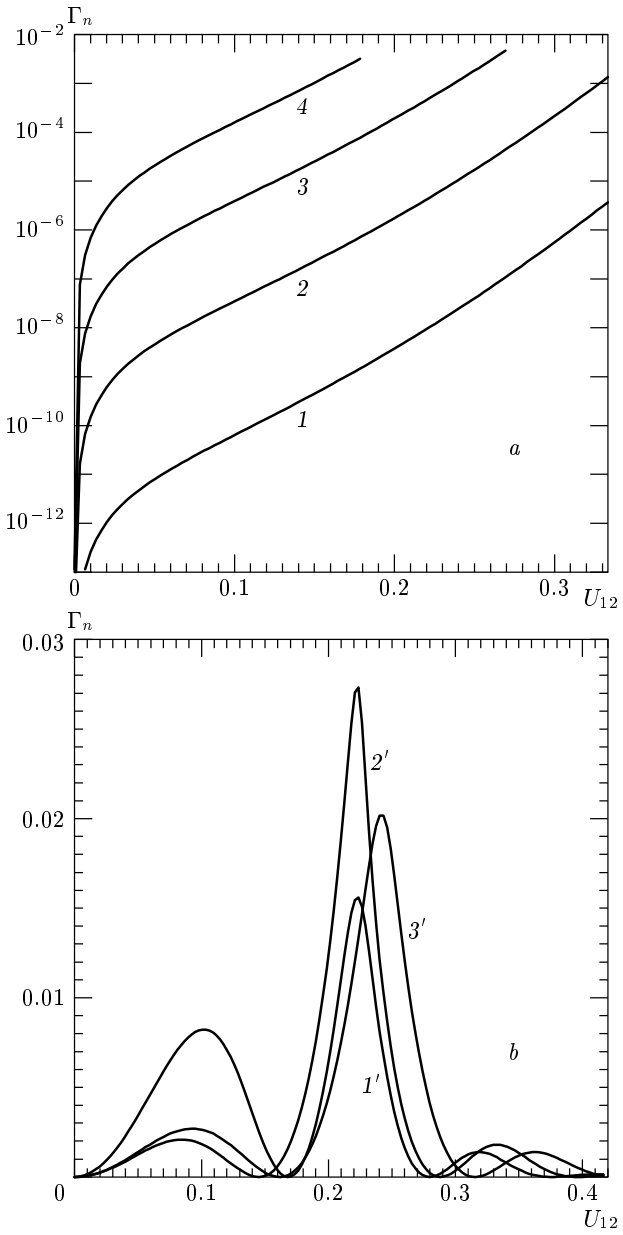

Fig. 13. Γ_n versus U_{12} for the quasistationary states at the diabatic potentials $(1+X)^2/2$ and $1/2-X$ crossing; (a) *1–4* are the level energies 0.042, 0.125, 0.208, and 0.292 for the lower adiabatic potential, (b) *1′–3′* are the level energies 0.625, 0.708, 0.792 for the upper adiabatic potential

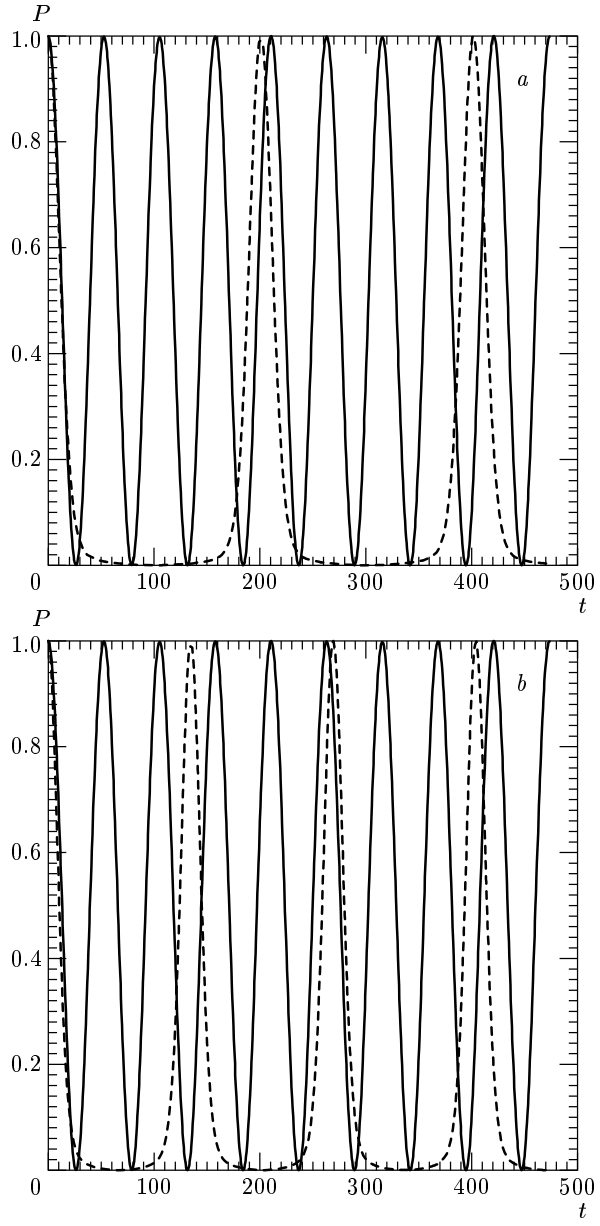

Fig. 14. Survival probability for the localized $n=0$ state; (a) $b=1500$, dashed lines $U_{12}=0.15$, solid lines $U_{12}=0.21$; (b) $b=1500$, dashed lines $U_{12}=0.28$, solid lines $U_{12}=0.21$

the aim to study the crossover behavior from coherent to incoherent tunneling with the increase of the parameter b; the larger b is, the larger the density of final states becomes. The criterion for coherent–incoherent crossover behavior found in [64] is based on comparison of the transition matrix elements and the interlevel spacings in the final state. A similar criterion should hold for LZ level crossing problem, but the tunneling transition matrix elements must then be multiplied by the small adiabatic factor. Therefore, the coherent–incoherent tunneling crossover region moves to the denser density of final states, and the larger U_{12} is, the smaller the region for incoherent tunneling becomes.

A totally different situation occurs for highly ex-

cited states. In the diabatic limit, the transition matrix element increases with the Massey parameter ν, and therefore at a given b value, the system moves to more incoherent behavior. In the adiabatic limit, the transition matrix element is exponentially small and coherence of the inter-well transitions should be restored. But because the matrix elements are oscillating functions of U_{12} for the intermediate range of this coupling, coherent–incoherent tunneling rates are also nonmonotonically varying functions. These unusual phenomena are illustrated in Fig. 14, where we show time dependence of the survival probability P for the initially prepared state $n = 0$ localized in the left well.

8. CONCLUSIONS

We have reconsidered a very basic subject, the LZ problem. Currently, about 100 publications per year are related to the LZ problem. Clearly, it is impossible to give a complete analysis of the achievements in this field. Our aim was therefore only to show some recent trends and our new results, to help beginners and experts find cross-references between the many physical phenomena related to the LZ problem. The problem was first addresses long ago, and many results, already classic, are now known from textbooks [1, 37]. Although exact quantum-mechanical calculations are still prohibitively difficult, many important results have been obtained in the framework of the WKB approach [1–65]. The accuracy of the modified WKB methods can be improved considerably; we note, e.g., [30], where the standard WKB was extended by the inclusion of a special type of trajectories in the complex phase plane such that the semiclassical motion along these trajectories is described by the Weber functions. This method, ascending to Landau [1], is equivalent to the appropriate choice of the integration path around the turning point. It appears to be quite accurate for the tunneling and over-barrier regions, where the characteristic fourth-order polynomial (see (4.16)) can be reduced to a second-order polynomial (two pairs of roots are nearly degenerate). But even in this case, some corrections have been found in [23–25] that cannot be neglected. In the intermediate energy region, where all four roots are noticeably different, the method becomes invalid. In addition, the choice of these additional special trajectories (which must be included to improve the accuracy of the WKB method near the barrier top) depends on a detailed form of the potential far from the top, and therefore a nonuniversal procedure is to be performed from the very beginning in each particular case.

We believe we are the first to explicitly addresses the problem of the behavior in the intermediate energy region. In all previous publications, this region was considered as a very narrow and insignificant one, or at most, the results were obtained by a simple interpolation from the tunneling region (with a monotonic decay of the transition probability) to the over-barrier region (with oscillating behavior). The fact is that classical trajectories can be separated into two classes, «localized» and «delocalized», in the following sense. If the energy is sufficiently close to the minimum or maximum of the potentials, the trajectories can be called confined, because they are determined by the universal features of the potentials in the vicinity of these extremal points. Evidently, this is not the case in the intermediate energy region. In this paper, we have found that contrary to a common belief, the instanton trajectory is a rather simple object and can be explicitly computed even for the intermediate energy region.

Within the framework of the instanton approach, we present a full and unified description of the $1D$ LZ problem, which can very often be quite a reasonable approximation for real systems. Because different approaches have been proposed to study the LZ problem, we develop a uniform and systematic procedure for handling the problem. We reproduced all the known results for tunneling and over-barrier regions, and studied the intermediate energy region. Specifically, we applied our approach to the Born–Oppenheimer scheme, formulated the instanton method in the momentum space, and presented all the details of the LZ problem for two electronic states also using the instanton description of the LZ problem in the coordinate space. Neglecting higher-order space derivatives, we found asymptotic solutions; using the adiabatic–diabatic transformation, we then matched the solutions in the intermediate region. Based on these results, we derived the complete scattering matrix for the LZ problem, the quantization rules for crossing diabatic potentials. Our results can be applied to several models of level crossings that are relevant in the interpretation and description of experimental data on spectroscopy of nonrigid molecules and on other systems undergoing crossing and relaxation phenomena.

We also note that in spite of a sufficiently long history of the LZ phenomena, the study is still in an accelerating stage, and a number of questions remain to be clarified (we mention only several new features of the phenomena that attracted attention recently, like the LZ interferometry for qubits [74], LZ theory for

Bose–Einstein condensates [75], and multi-particle and multi-level LZ problems [76–79]). Much of the excitement arises from the possibility of discovering novel physics beyond the semiclassical paradigms discussed here. For example, we found in Secs. 2 and 3 that the wave functions of nuclei moving along periodic orbits acquire geometric phases (the effect is analogous to the Aharonov–Bohm effect [38], but is related not to external magnetic fields, but to nonadiabatic interactions). The relation between the two phenomena, the geometric phases and the periodic orbits, can be established using the Lagrangian (instead of Hamiltonian) formulation of the problem, which enables taking the time dependence of the adiabatic process under consideration into account explicitly, using propagator technique [34–36] (also see, e.g., [4, 43]). Properly handling these aspects is beyond the scope of our work, however. Further experimental and theoretical investigations are required for revealing the detailed microscopic and macroscopic properties of different LZ systems.

In the fundamental problems of chemical dynamics and molecular spectroscopy, transitions from the initial to final states can be treated as a certain motion along the potential energy surfaces of the system under consideration. These surfaces are usually determined within the Born–Oppenheimer approximation (see Sec. 2). However, the approximation becomes inadequate for the excited vibrational states when their energies are of the order of the electronic inter-level energy spacing or near the dissociation limit. In both cases, nonadiabatic transitions should be taken into account, and most of the nonradiative processes occur owing to this nonadiabaticity. Typical examples investigated in [80] are the so-called pre-dissociation, singlet–triplet or singlet–singlet conversion, and vibrational relaxation phenomena.

Slow atomic collisions provide other examples of nonadiabatic transitions between electronic states, where the time dependence of the states is determined by distance and by the relative velocity of the colliding particles [33]. Some examples of nonadiabatic transitions relevant in semiconductor physics can be found in [81], those pertaining to nuclear or elementary particle physics in [82], and those relevant in laser or nonlinear optic physics in [83–86]. The latter topic is interesting not only in its own right, but also as an illustration of novel and fundamental quantum effects related to the LZ model. The off-diagonal electronic state interactions arise from the dipole forces in this case. For relatively short laser pulses, this leads to the time-dependent LZ problem for two electronic states, considered in our paper in detail (also see the laser optic formulation in [83–85]). The probability to find the system in the upper state after a single resonant passage can be computed in the framework of the LZ model. This is related to one important aspect of the LZ problem, namely dissipative and noisy environments. When external actions (e.g., fields) driving LZ transitions are reversed from large negative to large positive values, the dissipation reduces tunneling and the system remains in the ground state, or in other words, the thermal excitation from the ground state to the excited one suppresses such adiabatic transitions. But for the field swept from the resonance point, the tunneling probability becomes larger in the presence of dissipation (see, e.g., [67]). The increasing precision of experimental tests in the femtosecond laser pulse range enables one to excite well-defined molecular states and to study their time evolution using the second probing laser beam [17].

This paper was supported in part by RFFR Grants. One of us (E. K.) is indebted to INTAS Grant (under № 01-0105) for partial support.

REFERENCES

1. L. D. Landau and E. M. Lifshits, *Kvantovaya Mekhanika (nerelyativistskaya theoriya)*, Nauka, Moskva (1989).
2. E. E. Nikitin, Optika i Spectroskopiya **13**, 761 (1962); Disc. Farad. Soc. **33**, 14 (1962).
3. Yu. N. Demkov, Zh. Eksp. Teor. Fiz. **45**, 195 (1963).
4. G. Hertzberg and H. C. Longuet-Higgins, Disc. Farad. Soc. **35**, 77 (1963).
5. E. E. Nikitin, Chem. Phys. Lett. **2**, 402 (1968).
6. M. S. Child, Adv. Atom. Mol. Phys. **14**, 225 (1978).
7. H.-W. Lee and T. F. George, Phys. Rev. A **29**, 2509 (1984).
8. S. Griller and C. Gonera, Phys. Rev. A **63**, 052101 (2001).
9. A. M. Dykhne, Zh. Eksp. Teor. Fiz. **38**, 570 (1960).
10. A. M. Dykhne, Zh. Eksp. Teor. Fiz. **41**, 1324 (1961).
11. A. M. Dykhne and A. V. Chaplik, Zh. Eksp. Teor. Fiz. **43**, 889 (1962).
12. G. V. Dubrovskii, Zh. Eksp. Teor. Fiz. **46**, 863 (1964).
13. L. P. Kotova, Zh. Eksp. Teor. Fiz. **55**, 1375 (1968).

14. P. Pechukas, T. F. George, and K. Morokuma, J. Chem. Phys. **64**, 1099 (1976).

15. J. P. Davis and P. Pechukas, J. Chem. Phys. **64**, 3129 (1976).

16. J.-T. Hwang and P. Pechukas, J. Chem. Phys. **67**, 4640 (1977).

17. B. M. Garraway and S. Stenholm, Phys. Rev. A **45**, 364 (1992).

18. K.-A. Suominen, Phys. Rev. A **45**, 374 (1992).

19. N. V. Vitanov and B. M. Garraway, Phys. Rev. A **53**, 4288 (1996).

20. N. V. Vitanov, Phys. Rev. A **59**, 988 (1999).

21. N. V. Vitanov and K.-A. Suominen, Phys. Rev. A **59**, 4580 (1999).

22. J. B. Delos, W. R. Thorson, and S. K. Knudson, Phys. Rev. A **6**, 709 (1972).

23. C. Zhu, H. Nakamura, N. Re, and V. Aquilanti, J. Chem. Phys. **97**, 1892 (1992); C. Zhu and H. Nakamura, ibid **97**, 8497 (1992).

24. C. Zhu and H. Nakamura, J. Chem. Phys. **98**, 6208 (1993).

25. C. Zhu and H. Nakamura, J. Chem. Phys. **101**, 4855 (1994), ibid **101**, 10630 (1994).

26. V. A. Benderskii, D. E. Makarov, and C. A. Wight, *Chemical Dynamics at Low Temperatures*, Wiley-Intersci., New York (1994).

27. V. A. Benderskii, E. V. Vetoshkin, and H. P. Trommsdorf, Chem. Phys. **244**, 273 (1999).

28. V. A. Benderskii and E. V. Vetoshkin, Chem. Phys. **257**, 203 (2000).

29. V. A. Benderskii, E. V. Vetoshkin, and E. I. Kats, Zh. Eksp. Teor. Fiz. **122**, 746 (2002).

30. V. L. Pokrovskii and I. M. Khalatnikov, Zh. Eksp. Teor. Fiz. **40**, 1713 (1961).

31. B. K. Bykhovskii, E. E. Nikitin, and M. Ya. Ovchinnikova, Zh. Eksp. Teor. Fiz. **47**, 750 (1965).

32. V. M. Akulin and W. P. Schleich, Phys. Rev. A **46**, 4110 (1992).

33. E. E. Nikitin and S. Ya. Umanskii, *Theory of Slow Atomic Collisions, Springer Series in Chem. Phys.* **30**, Springer, Berlin (1984).

34. W. H. Miller and T. F. George, J. Chem. Phys. **56**, 5637 (1972).

35. R. K. Preston, C. Sloane, and W. H. Miller, J. Chem. Phys. **60**, 4961 (1974).

36. F. J. McLafferty and T. G. George, J. Chem. Phys. **63**, 2609 (1975).

37. J. C. Slater, *Quantum Theory of Molecules and Solids*, Vol. 1, McGraw Hill Book Company, New York (1963).

38. Y. Aharonov and D. Bohm, Phys. Rev. **115**, 485 (1959).

39. C. A. Mead, J. Chem. Phys. **78**, 807 (1983).

40. M. V. Berry, Proc. Roy. Soc. London A **392**, 451 (1984).

41. M. Wilkinson, J. Phys. A **17**, 3459 (1984).

42. M. V. Berry, J. Phys. A **18**, 15 (1985).

43. H. Kuratsui and S. Ida, Progr. Theor. Phys. **74**, 439 (1985).

44. M. V. Berry, J. Mod. Opt. **34**, 1401 (1987).

45. J. Vidal and J. Vudka, Phys. Rev. A **44**, 5383 (1991).

46. A. Mustafazadeh, Phys. Rev. A **55**, 1653 (1997).

47. R. F. Fox and P. Jung, Phys. Rev. A **57**, 2339 (1998).

48. C. A. Mead, Rev. Mod. Phys. **64**, 51 (1992).

49. Y. Aharonov and J. Anandan, Phys. Rev. Lett. **58**, 1593 (1987).

50. J. Samuel and R. Bhachdari, Phys. Rev. Lett. **60**, 2339 (1988).

51. N. Mukunda and R. Simon, Ann. Phys. **228**, 20 (1993).

52. M. V. Berry and J. M. Robbins, Proc. Roy. Soc. A **442**, 659 (1993).

53. J. Moody, A. Shapere, and F. Wilczek, Phys. Rev. Lett. **56**, 893 (1987).

54. D. Suter, G. C. Chingas, R. A. Harris, and A. Pines, Mol. Phys. **61**, 1327 (1987).

55. F. Gaitan, Phys. Rev. A **58**, 1665 (1998).

56. M. Baer, S. H. Lin, A. Alijah, S. Adhikari, and G. D. Billing, Phys. Rev. A **62**, 032506 (2000).

57. J. Heading, *An Introduction to Phase-Integral Methods*, Wiley-Intersci., London (1962).

58. A. M. Polyakov, Nucl. Phys. B **129**, 429 (1977).

59. S. Coleman, *Aspects of Symmetry*, Cambridge Univ. Press, Cambridge (1985).

60. M. S. Child, Mol. Phys. **20**, 171 (1971).

61. M. S. Child, J. Mol. Spect. **53**, 280 (1974).

62. T. Holstein, Phil. Mag. **37**, 49 (1978).

63. G. Stick and M. Thoss, Phys. Rev. Lett. **78**, 578 (1997).

64. V. A. Benderskii and E. I. Kats, Phys. Rev. E **65**, 036217 (2002).

65. N. T. Maintra and E. J. Heller, Phys. Rev. A **54**, 4763 (1996).

66. Y. Kayanuma and H. Nakayama, Phys. Rev. B **57**, 14553 (1999).

67. K. Saito and Y. Kayanuma, Phys. Rev. A **65**, 033407 (2002).

68. M. V. Fedoryuk, Dokl. Akad. Nauk **158**, 540 (1964).

69. M. V. Fedoryuk, Dokl. Akad. Nauk **162**, 287 (1965).

70. M. V. Fedoryuk, Uspekhi Matem. Nauk **21**, 1 (1966).

71. A. Erdelyi, W. Magnus, F. Oberhettinger, and F. G. Tricomi, *Higher Transcendental Functions*, Vol. 1–3, McGraw Hill, New York (1953).

72. F. W. J. Olver, *Asymptotics and Special Functions*, Academ. Press, New York (1974).

73. F. W. J. Olver, J. Res. NBS **63** B, 131 (1959).

74. A. V. Shytov, D. A. Ivanov, and M. V. Feigelman, E-print archives, cond-mat/0110490.

75. V. A. Yurovsky, A. Ben-Reuven, and P. S. Julienne, Phys. Rev. A **65**, 043607 (2002).

76. V. L. Pokrovsky and N. A. Sinitsyn, Phys. Rev. B **65**, 153105 (2002).

77. N. A. Sinitsyn, E-print archives, cond-mat/0212017.

78. Y. N. Demkov and V. N. Ostrovsky, Phys. Rev. A **61**, 032705 (2000).

79. D. A. Garanin and E. M. Chudnovsky, Phys. Rev. B **65**, 094423 (2002).

80. H. Eyring, S. H. Lin, and S. M. Lin, *Basic Chemical Kinetics*, Wiley Intersci., New York (1983).

81. Yu. A. Bychkov and A. M. Dykhne, Zh. Eksp. Teor. Fiz. **21**, 783 (1965).

82. S. Toshev, Phys. Lett. B **198**, 551 (1987).

83. J. M. Juan and T. F. George, J. Chem. Phys. **68**, 3040 (1978).

84. A. D. Bandrauk and G. Turcott, J. Chem. Phys. **77**, 3867 (1982).

85. H. W. Lee and T. F. George, Phys. Rev. A **35**, 4977 (1987).

86. V. M. Akulin and N. V. Karlov, *Intense Resonant Interactions in Quantum Electronics*, Springer, Berlin (1992).